A Bi-Level Optimization Strategy for Electric Vehicle Retailers Based on Robust Pricing and Hybrid Demand Response

Weiqi Meng[1], Dongran Song[1,*], Liansheng Huang[2,3,**], Xiaojiao Chen[2], Jian Yang[1], Mi Dong[1], M. Talaat[4,5]

[1]School of Automation, Central South University, Changsha, China

[2]Institute of Plasma Physics, Chinese Academy of Sciences, Hefei, China

[3]University of Science and Technology of China, Hefei, China

[4]Electrical Power and Machines Department, Faculty of Engineering, Zagazig University, P.O.44519, Zagazig, Egypt

[5]Faculty of Engineering and Technology, Egyptian Chinese University, P.O. 11787, Cairo, Egypt

Abstract: The high penetration of electric vehicles (EVs) poses both opportunities and challenges for power systems. EV retailers, playing a critical role in the demand response mechanism, face market risks caused by uncertainties in electricity consumption and prices. To address the operational issues of large-scale EVs and tap the potential of EV retailers, a temporal and spatial domain-based optimization strategy is proposed, which is implemented on bi-level (referring to transmission and distribution grid networks). First, a physical scheduling model of the grid is established, consisting of a novel hybrid demand response mechanism considering the incentives of EV retailers and the retail electricity price of EV users, and a new robust retail electricity pricing strategy handling the uncertainties of EV behavior and the electric market. Then, a bi-level optimization strategy is presented: at the upper level, in the transmission network, based on the robust pricing strategy, a unit commitment model that coordinates the hybrid demand response with other distributed energy resources is designed to optimize load periods of EVs in the time domain; at the lower level, in the distribution network, an optimal power flow model is proposed to spatially dispatch the location of EV loads. The impacts of retail price profile, EV penetration, hybrid demand response mechanism, and EV load location are analyzed in ten tests using the IEEE 33 distribution network. Simulation results indicate that the robust pricing strategy can effectively handle uncertainties, the integration of the hybrid demand response mechanism into scheduling can ensure the benefits of all participants, and the bi-level optimization strategy can accommodate distributed energy resources temporally and spatially.

Keywords: Electric vehicle retailer; Transmission and Distribution Networks (TDNs); robust pricing; demand response (DR); Unit Commitment; Optimal Power Flow

* **Co-correspondence**

Dongran Song, email: songdongran@csu.edu.cn; Liansheng Huang, email: huangls@ipp.ac.cn

Dongran Song*, Liansheng Huang** The two authors have the same contribution to this study.

Nomenclature

Abbreviations

PV	Photovoltaic generation
DERs	Distributed energy resources
EVs	Electric vehicles
TDNs	Transmission and distribution networks
UC	Unit commitment
OPF	Optimal power flow
IBDR	Incentive-based demand response
PBDR	Price-based demand response
PSO	Particle swarm optimization
V2G	Vehicle-to-grid
AA-CAES	Advanced adiabatic compressed air energy storage
LSTM	Long Short-Term Memory
XGBoost	eXtreme Gradient Boosting
TSO	Transmission system operator
DSOs	Distribution system operators
MCS	Monte Carlo simulation
MINLP	Mixed-integer nonlinear programming
DR	Demand response
MP	Main problem
SP	Sub problem
ES	Energy storage
CC&G	Column-and-constraint generation
MIQP	Mixed-integer quadratic programming
DLMP	Distribution locational marginal price
MILP	Mixed integer linear program
MIP-RS	Mixed-integer programming robust strategy
MINP-RS	Mixed-integer nonlinear programming robust strategy
PSO-RS	Particle swarm optimization robust strategy

Variables

$\boldsymbol{S}$	Number of wind power scenarios
$\boldsymbol{T}$	Total number of time intervals
$\boldsymbol{N}_{\mathrm{g}}$	Total number of thermal units
$\boldsymbol{N}_{w}$	Total number of wind units
$\boldsymbol{N}_{pv}$	Total number of PV units
$\boldsymbol{U}_{t}^{s}$	Revenue via selling electricity to EV owners
$\boldsymbol{C}_{Demond}$	Compensation cost of IBDR mechanism
$\sigma_{n,t}^{EV}$	Unit utility of EV_n at time t
G_i^h, G_i^c	The hot and cold start cost of unit i
$X_{i,t}^{\mathrm{off}}$	Continuously off-line time of unit i at time t
T_i^{off}	Minimal shut-down time of unit i
T_i^c	Cold start time of unit i
$N_{c,t}^s, N_{d,t}^s$	Number of EVs schedule at time t in scenario $\boldsymbol{s}$
P_c, P_d	The charging and discharging power of EVs
Δt	Length of time interval
C_w, C_{pv}	Punish price of wind and PV curtailment
$\Delta P_{w,s}^s, \Delta P_{pv,s}^s$	Wind and PV power curtailment of at time t in scenario $\boldsymbol{s}$
$\boldsymbol{\pi}$	Retail electricity prices of EVs
$\boldsymbol{J}$	Total number of EV retailers
$\boldsymbol{u}_{i,t}$	Operation status of unit i at time interval t
$\boldsymbol{C}_{\boldsymbol{e}}$	Punish price of PM2.5 emission
$\boldsymbol{w}$	The amount of power reduction (/MW)
$\boldsymbol{u}$	Incentive obtained (/￥)
$\boldsymbol{\gamma}$	The "value of power interruptibility"
$\boldsymbol{K}_{\mathbf{1}}, \boldsymbol{K}_{\mathbf{2}}$	Cost coefficients of EV retailers
$\boldsymbol{\theta}_{\boldsymbol{j}}$	The willingness to curb power for EV retailer$\boldsymbol{j}$
$\boldsymbol{CM}_{\boldsymbol{j}}$	Daily limit of interruptible power for EV retailer$\boldsymbol{j}$ (WMh)
$\boldsymbol{UB}$	TDNs' total compensation budget
$\boldsymbol{P}_{\boldsymbol{b},t}^{\boldsymbol{Da}}$	Day ahead electricity purchased by the operator at time t
$\boldsymbol{\pi}_t$	Retail electricity price at time t
$\boldsymbol{P}_{\boldsymbol{b},t,o}^{\boldsymbol{Re}}, \boldsymbol{P}_{s,t,o}^{\boldsymbol{Re}}$	EV retailer’s real-time electricity plan under the DR of EVs at time t in scenario $\boldsymbol{o}$
$\boldsymbol{P}_{ch,t,o}^{\boldsymbol{ESS}}, \boldsymbol{P}_{dis,t,o}^{\boldsymbol{ESS}}$	Power schedule of the energy storage system at time t in scenario $\boldsymbol{o}$
$p_{ch,n,t}^{EV}, p_{dis,n,t}^{EV}$	The charging and discharging schedule for EV_n
$\boldsymbol{S}_{\boldsymbol{t},\boldsymbol{o}}^{\mathbf{ESS}}$	Battery power of the energy storage system at time t in scenario $\boldsymbol{o}$
$\alpha_i, \beta_i, \gamma_i$	Coal consumption coefficients of unit i
$U_{p,t}$	Voltage of node p at time t
U_{ref}	Expected voltage of the node
$\boldsymbol{k}$	The k-$_{th}$ iteration
$\boldsymbol{x}, \boldsymbol{\pi}$	Decision variables of the first stage
$\boldsymbol{y}_o$	Decision variables of the second stage
$\boldsymbol{\rho}_0$	Empirical distribution of uncertain variables
$\boldsymbol{\rho}$	A vector representing $\boldsymbol{\rho}_0$
o	Real-time DLMP scenarios
$\boldsymbol{X}, \boldsymbol{\Pi}, \boldsymbol{Y}, \boldsymbol{\mathcal{R}}, \mathcal{O}, \mathcal{K}$	The variable space of $\boldsymbol{x}, \boldsymbol{\pi}, \boldsymbol{y}, \boldsymbol{\rho}, o, \boldsymbol{k}$
v_o	Occurrence probability of scenario o
$\boldsymbol{a}$	Coefficient vectors

$\boldsymbol{C_{AA-CAES}}$	The unit power purchase cost of the AA-CAES	n	Number of clusters for EVs
$P_{i,t}^{s}$	Output of unit i at time t in scenario $\boldsymbol{s}$	$\boldsymbol{A}, \boldsymbol{B}, \boldsymbol{C}, \boldsymbol{E}_n, \boldsymbol{M}$	Coefficient matrices
a_i, b_i, c_i	Positive fuel cost coefficients of unit i	b_o	Coefficient vector corresponding to scenario o
$\boldsymbol{F}_i(\boldsymbol{P}_{i,t}^{s})$	Fuel costs of the thermal units	$\boldsymbol{c}_n$	Coefficient vector corresponding to EV_n
$\boldsymbol{E}_i(\boldsymbol{P}_{i,t}^{s})$	The PM2.5 emission costs of the thermal units	$\mathcal{N}^{\mathrm{EV}}$	Collection of EVs
$\boldsymbol{G_{start-up}}$	Start-up cost of the thermal units	$\boldsymbol{\rho}_{k^*}$	Worst-case EVs set returned by SP at the k-$_{th}$ iteration
$\boldsymbol{W}_t^{s}$	Wind and PV curtailment costs	$\boldsymbol{y}_{o,k}$	The newly introduced variable associated with $\boldsymbol{\rho}_{k^*}$
$\boldsymbol{E}\{\cdot\}$	Mathematical expectation	$\boldsymbol{x}_{k^*}$	Value of purchased electricity at the k-$_{th}$ iteration
$\boldsymbol{P}_{ro}{}^{\boldsymbol{s}}$	Probability of scenario $\boldsymbol{s}$	$\boldsymbol{\pi}_{ch,k^*}^{T}, \boldsymbol{\pi}_{dis,k^*}^{T}$	The charging and discharging retail price at the k-$_{th}$ iteration
$\boldsymbol{\ell}$	Weight percentage of ash in the coal (%)	$\boldsymbol{z}_{k^*}$	Power schedule of EVs at the k-$_{th}$ iteration
$\boldsymbol{\omega}$	Conversion factor of total ash to PM2.5 (%)	F, Q	An auxiliary variable introduced
$\boldsymbol{\eta}$	Emission reduction efficiency (%)	$\boldsymbol{e}_n, \boldsymbol{m}$	Vector of EV_n
$C_{AA-CAES}^{Rp}$	Positive standby market cost of AA-CAES	$\zeta_n, \boldsymbol{\partial}_o, \mathcal{E}_o$	Dual variables
$C_{AA-CAES}^{\boldsymbol{Rn}}$	Negative standby market cost of AA-CAES	r_{pq}	Resistance of branch pq
$C_{AA-CAES}^{G}$	Positive energy market cost of AA-CAES	$I_{pq,t}$	Current flowing through branch at time t
$C_{AA-CAES}^{C}$	Negative energy market cost of AA-CAES	$\boldsymbol{\phi}$	Set of branches
H_i^{off}	Transition hour	N_{branch}	Number of distribution network branches
$\varrho_{ch}^{EV}, \varrho_{dis}^{EV}$	The charging and discharging efficiencies of EVs		

1 Introduction

In recent years, the utilization of distributed energy resources (DERs) has increased, and many efforts have been made to integrate them into power systems [1]. As a typical form of DERs, electric vehicles (EVs) are seen as gaining importance due to their environmental benefits [2]. The large-scale integration of EVs into the power grid can impose substantial strain on both transmission and distribution networks (TDNs), leading to concerns about potential voltage fluctuations and peak load management [3]. To mitigate these impacts, encouraging the active participation of EVs in energy management is recommended [4].

The increasing uncertainty in electricity market pricing, coupled with the rising prevalence of flexible loads like EVs and renewable energy, has significantly complicated both transmission and distribution network dynamics [5]. On the one hand, the stringent power quality standards and the need for robust power system operation are posing fresh challenges for both transmission and distribution system operators, especially in the context of high EV penetration [6]. On the other hand, consumers are becoming more conscious of grid tariffs and exploring diverse energy procurement methods [7], such as the adoption of demand response mechanisms [8]. The integrated optimization of TDNs necessitates the seamless coordination of both power systems and EVs to enhance the efficiency, reliability, and stability of power grids. As EVs become more widespread and demand response (DR) technologies advance, the coordination of TDNs with large-scale EVs faces new challenges, which can be summarized into three key aspects: the precise scheduling model, economic strategies, and the co-optimization of TDNs and EVs [9].

For the precise scheduling model of TDNs with EVs, it represents how the scheduling of large-scale EVs is integrated into the scheduling model of the TDNs. There are currently numerous modeling tools available [10]. Ref. [11] employs a clustered unit commitment (UC) model to accurately describe the flexible supply capability of aggregated units. Ref. [12] establishes a probabilistic coordination model for TDNs to address the uncertainty of large-scale renewable energy grid connections. Most existing models are developed from the perspective of either the transmission grid or the distribution grid individually, and few of them fully consider essential details, such as the demand response of both EV retailers and EV users. Ref. [13] emphasizes that the fundamental challenge in the development of TDNs is how to involve the DR mechanism of large-scale EVs in the process. Based on this, research on demand response mechanisms between EVs and TDNs is a new trend in the context of precise scheduling models. To meet the stability of the power system with large-scale distribution energy resources, the authors of [14] design an incentive-based demand response (IBDR) mechanism for EV retailers, which is solved by particle swarm optimization (PSO). A robust economic dispatch strategy for the low-carbon power system considering price-based demand response (PBDR) and vehicle-to-grid (V2G) is proposed in [15]. In [16], a method for time-of-use tariff rate estimation is proposed for optimal DR management by EVs. In [17], an EV fast charging station is designed by considering the uncertainty of renewable energy and the PBDR. Combining the theory of reinforcement learning, an IBDR mechanism for EV users is designed in [18]. A similar IBDR mechanism for end users is designed in [19], while the optimization is modeled as a mixed-integer linear program. Besides the above single DR mechanism for EVs, a hybrid DR mechanism combining real-time pricing and real-time incentives is proposed in [20]. Without the management of EV retailers, some EV users may be apathetic about the electricity price changes or incentives when continuously adjusting the load.

For the economic strategy of TDNs, it mainly represents how EV retailers, as intermediate units in the scheduling model, participate in the electricity market of the TDNs on behalf of EV users and how retail electricity prices are formulated to reflect the game between them and EV users, earning profit from price differences, and avoiding market risks [21]. The retail price of EV retailers is influenced by uncertain factors such as the high penetration of EV distribution and the electricity markets [22]. Existing relevant literature on pricing strategies can be mainly categorized into two types: distributed and centralized. Regarding the distributed pricing strategy, a distributed hierarchical transactive energy framework for EVs with DERs in distribution networks is designed in [23]. In [22], a hierarchical scheduling framework for all participants is established with a fair payment mechanism. To tackle uncertainties such as the electricity price, the authors of [24] design a hybrid stochastic-robust framework, in which a distributed optimization algorithm is used to coordinate the electricity exchange between aggregators. A two-stage distributionally robust optimization model to collaborate the EVs and distribution networks is proposed in [25], which considers the source-load uncertainties. Regarding the distributed pricing strategy, to achieve inter-biding cooperation, the authors of [26] propose a coordination mechanism for EV aggregators. To cope with the uncertainty of large-scale EVs, the authors of [27] formulate the EV scheduling plan as a constrained Markov decision process. To ensure the reliability and economy of the operation of the distributed networks, the authors of [28] propose a new electricity market clearing mechanism to charge both the power exchange and uncertain resources and coordinate distributed networks and microgrids. A robust day-ahead scheduling strategy for EV charging stations in the unbalanced distribution grid is proposed in [29], which focuses on reducing the unbalance of the grid. It should be noted that Ref. [30] proposes a robust pricing strategy for power retailers. However, Ref. [30] primarily focuses on the pricing mechanism of retail electricity between power retailers and end users. It neglects the potential for power retailers to actively participate in the energy management of TDNs. This gap could lead to suboptimal outcomes for TDNs, EV retailers and end users, and could cause a congestion problem [31].

For the co-optimization of TDNs and large-scale EVs, it represents how to comprehensively plan the charging time and charging locations of EVs and carry out coordinated optimization between the transmission grid and distribution networks based on the precise scheduling model. In recent years, some investigations have been carried out to optimize dispatch scheduling to benefit the distributed network, transmission network, and EVs. Ref. [32] proposes a robust power system co-optimization and scheduling scheme, considering the uncertainty of EVs and demand-side carbon emissions. To reduce both power systems and EV users operating costs, the authors of [33] design a model for managing EV charging behaviors and use reinforcement learning to solve the problem. Similarly, the authors of [34] design a multi-objective, multi-constraint optimization model for optimal dispatch scheduling of EVs in power systems. To meet the challenge of large-scale EVs in power systems, the authors of [35] propose a collaborative scheduling model for TDNs. To fully tap the flexibility of large-scale EVs in power systems, the authors of [36] design an optimized dispatching strategy for TDNs based on the dynamic electricity price mechanism of EVs. To promote the cooperation of EVs and power systems, an improved PSO algorithm is presented to manage the EVs' orderly scheduling in [37]. Similarly, a centrally coordinated EV scheduling strategy is proposed in [38]. A forecasting model for EV behaviors based on LSTM (Long Short-Term Memory) and XGBoost (eXtreme Gradient Boosting) is designed in [39], which aims to achieve cooperation with EVs and power systems. To support the grid by using EVs, the authors of [40] propose a double-layered intelligent energy management system for optimal EV aggregator integration. Similarly, a UC model for optimal V2G operation in power systems is designed in [41].

According to the presented explanations, analyses of previous relevant literature and the current work in the field of optimal scheduling of EVs in TDNs have been categorized in Table 1. While each of these works has significantly contributed to the field, they also exhibit certain weaknesses and limitations, as outlined below:

Table 1. A comparison between this work and previous publications.

Ref.	Uncertainty				Demand response			Retail pricing strategy		Participants			Model sol.
	Method	Units			IBDR	PBDR	Hybrid	Central	Distributed	Grid operator	EV Retailer	EV users	
		EV	Electricity Market	PV/Wind									
[12]	PR	×	×	✓	×	×	×	×	×	✓	×	×	ADMM
[14]	×	×	×	×	✓			×	×	×	✓	✓	PSO
[15]	RO	×	×	✓		✓		✓		✓	×	✓	MILP
[17]	PR	×	×	✓		✓		✓		✓	✓	×	PSO
[18], [19]	×	×	×	×	✓			✓		✓	×	×	MILP, ML
[20]	×	×	×	×			✓	✓		✓	✓	✓	ADMM
[22]	×	×	×	×		✓			✓	✓	✓	✓	ADMM
[23]	PO	✓	×	✓	×	×	×	×	×	✓	✓	×	ADMM
[24]	RO, PR	×	✓	✓		✓			✓	✓	✓	×	MIQCP
[25]	DRO	✓	×	✓	×	×	×	×	×	✓	×	✓	MILP
[26]	×	×	×	×		✓			✓	×	✓	×	MILP
[27]	PO	✓	×	×	×	×	×	×	×	×	×	✓	CMDP
[28]	RO	×	✓	✓	×	×	×		✓	✓	×	×	MILP
[29]	RO	✓	×	✓		✓		✓		✓	×	✓	MILP
[30]	RO	✓	✓	×		✓		✓		×	✓	✓	MILP
[32]	RO	✓	×	✓		✓		✓		✓	×	✓	MILP
[33]	PR	✓	×	✓	×	×	×	×	×	✓	✓	×	DQN
[34]	PR	✓	×	×	×	×	×	×	×	✓	×	✓	GSA-PSO
[35]	PO	✓	×	✓	×	×	×	✓		✓	×	✓	MILP
[36]	PO	×	×	✓	×	×	×	✓		✓	×	✓	MILP
[37], [39]	PR	✓	×	✓	×	×	×	×	×	✓	×	✓	PSO, BO
[40]	×	×	×	×	×	×	×	✓		✓	×	✓	GA, DE
[41]	×	×	×	×	×	×	×	×	×	×	×	✓	MILP
This paper	RO	✓	✓	✓	Hybrid			Central + Distributed		✓	✓	✓	MISOCP

*Note: *PR: Probabilistic, PO: Possibilistic, RO: Robust Optimization, DRO: Distributed RO, P: Probabilistic, MRO: Multi-objective robust optimization; IBDR: Incentive-based demand response, PBDR: Price-based demand response, Hybrid: Hybrid demand response; MILP: Mixed integer linear programming, CMDP: Constrained Markov decision process, MIQCP: Mixed-integer quadratic conic programming, MISOCP: Mixed-integer second-order cone programing, ADMM: Alternating direction method of multipliers, GSA: Gravitational search algorithm, PSO: Particle swarm optimization, GA: Genetic algorithm, DE: differential evolution, ML: Machine learning, DQN: Deep Q Network, BO: Bayesian optimization,*

(1) The DR mechanism of large-scale EVs is not fully considered in the previous precise scheduling model of TDNs [42]. EV scheduling schemes are optimized without the participation of EV users. Most previous grid-connected DR studies, such as the IBDR or PBDR, focus on the incentives for EV users or retailers separately but fail to consider grid operators, EV retailers, and users simultaneously. Since EVs are not responsible for the stability of the power system [43], the potential of the DR mechanism cannot be fully exploited without the coordination of the grid [20].

(2) In most investigations, the uncertainty of EV users and the electricity market are not considered in the economic strategies simultaneously, which cannot coordinate the payment mechanisms of EV retailers from the grid with the DR behavior of EVs [27]. The existing pricing strategies may expose retailers to market risks, leading to financial losses, and the Distribution locational marginal price (DLMP) is set mainly according to clearing prices without the participation of EV retailers.

(3) Extensive literature designs the optimal operation of EV retailers to improve efficiency but does not consider both the transmission and distribution operational constraints when deciding EV consumption patterns [36]. With the high penetration of EVs in distribution networks, the sustainable and economic co-optimization of TDNs and EVs is difficult due to differences in optimization region and time scale [44]. Few studies consider the flexibility of DERs, such as EVs and renewable energy, simultaneously, which makes it easy to aggravate the peak-valley difference of TDNs after integrated DR [41]. Furthermore, most articles have ignored the mobility of EVs between different nodes of the transportation system, such as residential, commercial, and official [34].

To fill the above research gap, a bi-level optimization schedule for large-scale EVs in TDNs is proposed in this work, which tends to better tap the potential value of EV retailers in TDNs by jointly considering a hybrid DR mechanism and a robust pricing strategy for EV retailers. In contrast to [25], this study introduces a novel market mechanism encompassing both the DR mechanism and pricing strategy. Unlike Ref. [26] and Ref. [30], a two-stage robust pricing strategy is developed for EV retailers in this research, which does not necessitate precise probability distributions of random market prices. This comprehensive strategy considers various factors, including the DR of both EV users and retailers, day-ahead scheduling, and real-time energy management. Unlike the PBDR in [17] and the IBDR mechanism in [19], the proposed hybrid DR mechanisms aim to integrate both EV retailers and users into the energy management framework rather than focusing solely on minimizing grid fuel costs. Moreover, the decision model in [37] employs an artificial intelligence method, and [39] adopts a mixed integer linear program (MILP), both of which differ from the model presented in this study. In view of the above discussions, this work makes practical sense. Overall, the technical contributions of this study are threefold.

1) An innovative hybrid DR mechanism is established in the precise scheduling model of TDNs, combining both the IBDR of EV retailers and the PBDR of EV users. IBDR changes electricity usage by EV retailers from their normal consumption patterns in response to incentive payments designed to induce lower electricity use when system reliability is jeopardized. A Stackelberg game-based PBDR between EV retailers and EV users is developed to achieve an economic win-win situation. The proposed hybrid DR mechanism can protect privacy, enable the endogenous determination of market roles, and stabilize load fluctuations more effectively. The precise scheduling model of TDNs incorporates EVs, EV retailers, renewables, energy storage, and thermal units, innovatively.

2) A two-stage robust pricing strategy is proposed to address the retail electricity price setting problems for EV retailers, as an intermediate unit in the scheduling model, aiming to enhance both EV retailers' profitability

and EV users' satisfaction. In the first stage (day-ahead), EV retailers determine their retail prices, while EV users make decisions about their consumption patterns. The interaction between retail prices and EV users' DR is modeled using a Stackelberg game model. In the second stage (real-time), EV retailers make decisions regarding the operation of storage units and energy contracts in the electricity market. Considering the uncertainty in wholesale market prices, the energy dispatch in the second stage is formulated as a linear max-min problem associated with the worst-case market price realization.

3) A temporal and spatial domain-based bi-level optimization schedule for large-scale EVs in TDNs is designed at both the transmission grid level and the distribution grid level. Firstly, at the upper level, based on the hybrid DR mechanism and retail electricity price, a UC optimization model is established in the time domain to improve the economy of the whole power system by coordinating EVs with DERs. Secondly, at the lower level, an optimal power flow (OPF) optimization model is proposed to minimize the operational cost of the distribution grid by reasonable spatial allocating the total EV loads to each node at the distribution grid level. Both EV penetration and EV load location impacts are also analyzed.

The rest of this paper is organized as follows: Section 2 introduces the structure of the bi-level optimization strategy, which is based on the hybrid DR mechanism and robust pricing strategy of EV retailers. Case studies and results analysis are presented in Section 3. Finally, Section 4 provides the conclusion and future outlook.

2 Proposed bi-level optimization schedule

The proposed bi-level optimization schedule, illustrated in Fig. 1, consists of two levels of optimization: an upper-level UC optimization in the transmission system operator (TSO), optimizing load periods of large-scale EVs in the time domain; a lower-level OPF optimization problem in the distribution system operators (DSOs), optimizing the spatial distribution of EV charging and discharging loads.

At the upper transmission grid level, based on the lower-level robust pricing strategy and the hybrid DR mechanism, the time-domain UC optimization coordinates the charging and discharging schedule of EVs, EV retailers' DR power, advanced adiabatic compressed air energy storage (AA-CAES), renewable energy power, thermal generators, and basic load. EV charging and discharging behaviors are optimized in the temporal dimension to reduce the operating costs for units, EV charging costs, EV retailer DR costs, environmental pollution costs, AA-CAES power purchase/sale costs, unit start-up/shutdown costs, and renewable energy curtailment costs. The day-ahead UC model considers EV retailers' retail electricity price in DSOs, the scheduling of EVs based on the PBDR mechanism in TDNs, the EV retailers IBDR mechanism in DSOs, the parameters of AA-CAES and thermal units, wind/PV (Photovoltaic) power forecast curves, and daily load.

At the lower distribution network level, based on the upper-level optimization results, the spatial-domain OPF optimization solves the optimal location for EV charging and discharging, optimizing EV charging and discharging behaviors. Besides, a robust pricing strategy of the EV retailers, considering the uncertainty of EV users and the real-time electricity market, and hybrid DR mechanisms for EV users and EV retailers are proposed to determine the retail price and the EV retailers shedding of power, which are used for UC optimization at the upper level. The goal of lower-level optimization is to reduce network operating costs and voltage deviation. The real-time OPF model is proposed based on the power supply from the transmission system, the daily load demand in the distribution network, and the profile of EV charging and discharging.

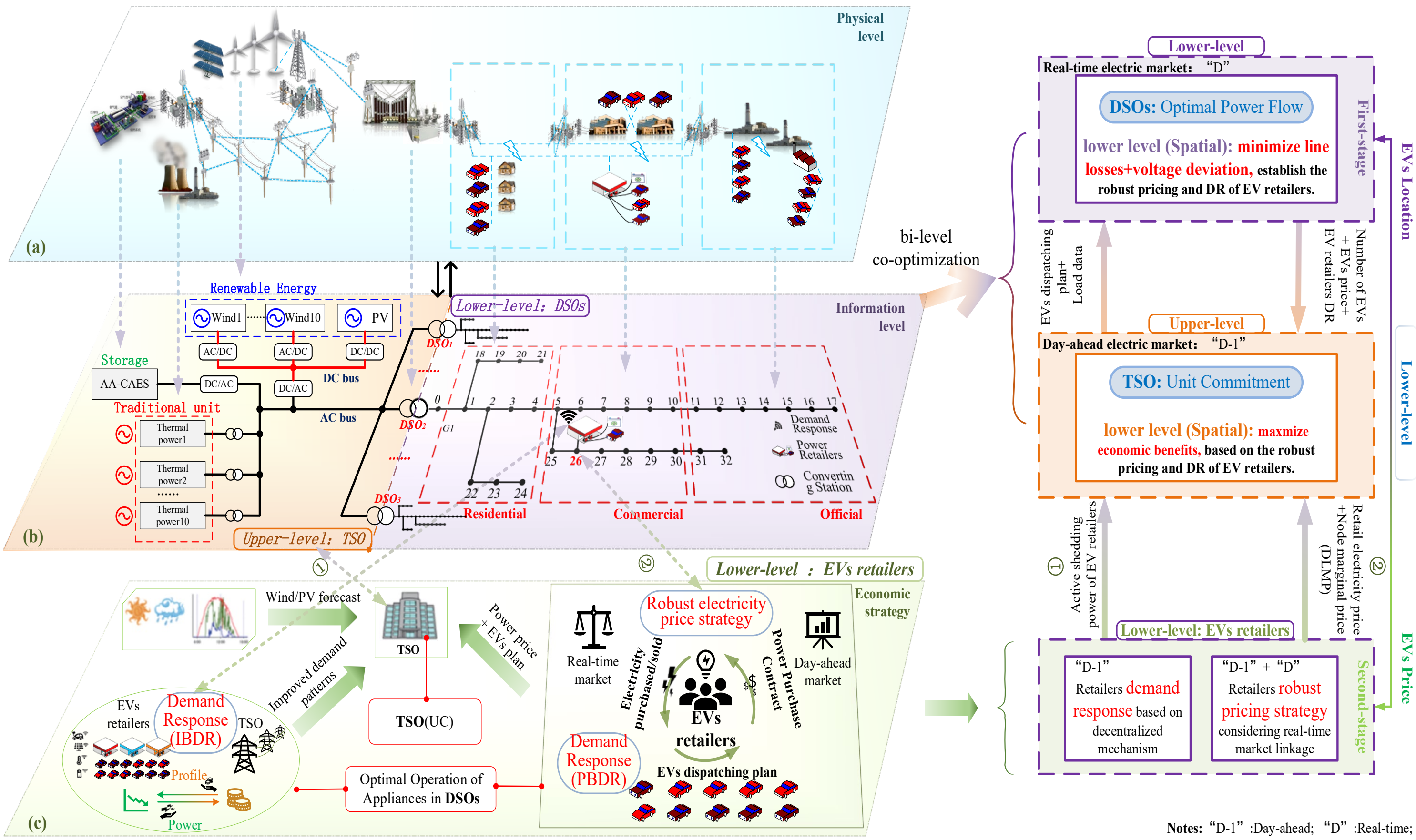

Fig.1. Process of bi-level optimization strategy for TDNs based on robust retail electricity price and DR.

2.1 The upper level of the proposed strategy

From the perspective of TDNs, the upper-level optimization is a UC problem. The objective of UC is to achieve the optimal scheduling of EV retailers, EVs, Wind, PV, AA-CAES, and thermal power units based on the hybrid DR plans of both EV retailers and EV users, to achieve better economic efficiency. In addressing the uncertainty of wind and PV power generation, the probabilistic method based on the Monte Carlo Simulation (MCS) is used for dealing with the uncertain parameters [45]. The scenarios of wind power are generated based on Monte Carlo simulation rather than thermal units. Distinct wind and PV power profiles are autonomously generated in accordance with the methodology outlined in Appendix A.2, thereby influencing various solutions in UC. Therefore, the output of units becomes intricately linked to the diverse scenarios of wind power. These scenarios are executed in isolation.

2.1.1 Optimal strategy for unit commitment

The UC plan is determined day-ahead, and units' output will be adjusted in response to varying scenarios. Consequently, the scenario-based day-ahead UC objective function of the upper-level optimization that maximizes the total expected operating profit for TDNs during the electricity trading process is denoted as follows:

$$min\, E\begin{Bmatrix} \sum_{t=1}^{T}(U_t^s + C_{Demond} + C_{AA-CAES}) \\ +\sum_{t=1}^{T}\sum_{i=1}^{N_g}\left(F_i\left(P_{i,t}^s\right) + E_i\left(P_{i,t}^s\right)\right) + \sum_{t=1}^{T} W_t^s \end{Bmatrix} + \left\{\sum_{t=1}^{T}\sum_{i=1}^{N_g} G_{start-up}\right\} \quad (1)$$

where, S represents the number of scenarios. T is the total number of time intervals. N_g is the total number of thermal units. $P_{i,t}^s$ represents the active power of unit i at time t in scenario s. U_t^s represents the revenue via selling electricity to EVs owners in scenario s. C_{Demond} denotes the compensation cost for encouraging EV retailers to participate into IBDR mechanism, which will be given a detailed explanation in the next section; $C_{AA-CAES}$ stands for the unit power purchase cost of the AA-CAES; $F_i(P_{i,t}^s), E_i(P_{i,t}^s), G_{start-up}$ and W_t^s stand for the fuel costs, the PM2.5 emission costs, the Start-up and Shut-down cost of the thermal units, the Wind and PV curtailment costs, respectively. $E\{\cdot\}$ denotes the mathematical expectation of all scenarios. The probability of scenario s is ${P_{ro}}^s$. The calculation of the expectation is: $E(X) = \sum_{i=1}^{N} (X_i \cdot P_{X_i})$, P_{X_i} is the probability of X_i.

$$U_t^s = \pi_{c,t} N_{c,t}^s P_c \Delta t - \pi_{d,t} N_{d,t}^s P_d \Delta t \tag{2}$$

$$F_i(P_{i,t}^s) = a_i + b_i P_{i,t}^s + c_i {P_{i,t}^s}^2 \tag{3}$$

$$E_i(P_{i,t}^s) = C_e \cdot u_{i,t} \cdot \ell \cdot \omega (1 - \eta/100)\left(\alpha_i + \beta_i P_{i,t}^s + \gamma_i P_{i,t}^{s2}\right)/10000 \tag{4}$$

$$G_{start-up} = G_{i,t} \cdot u_{i,t}(1 - u_{i,t-1}); G_{i,t} = \begin{cases} G_i^h & T_i^{off} < X_{i,t}^{off} \leqslant H_i^{off} \\ G_i^c & X_{i,t}^{off} > H_i^{off}, H_i^{off} = T_i^{off} + T_i^c \end{cases} \tag{5}$$

$$W_t^s = \sum_{w=1}^{N_w} C_w \Delta P_{w,t}^s + \sum_{p=1}^{N_{pv}} C_{pv} \Delta P_{pv,t}^s \tag{6}$$

$$C_{AA-CAES} = (C_{AA-CASE}^G - C_{AA-CASE}^C) + \left(C_{AA-CASE}^{Rp} + C_{AA-CASE}^{Rn}\right) \tag{7}$$

where, $\pi_{c,t}$ and $\pi_{d,t}$ are the retail electricity prices of EVs at time t, which are obtained by the robust electricity price strategy of EV retailers and the PBDR mechanism of EV users at the lower DSOs level. J is the total number of EV retailers. a_i, b_i and c_i are positive fuel cost coefficients of unit i. ℓ denotes the weight percentage of ash in the coal (%), and its default value is $20. \omega$ is the conversion factor of total ash to PM2.5 (%) and its default value is $5.1. \eta$ is emission reduction efficiency (%) and its default value is 99. $\alpha_i, \beta_i, \gamma_i$ are coal consumption coefficients of unit i. H_i^{off} denotes the transition hour, G_i^h is the hot start cost of unit i, G_i^c is the cold start cost of unit i, $X_{i,t}^{\text{off}}$ is the continuously off-line time duration of unit i at time t, T_i^{off} is the minimal shut-down time of unit i, and T_i^c is the cold start time of unit i. $N_{c,t}^s$ and $N_{d,t}^s$ are the number of EVs charging and discharging at time t in scenario s, respectively. P_{c} and P_d are the average charging and discharging power of EVs, respectively. Δt is the length of time interval, and its default value is 1. N_w and N_{pv} denote the total number of wind and PV generations, respectively. C_w and C_{pv} are the punish price of wind and PV curtailment, respectively. $\Delta P_{w,t}^s$ and $\Delta P_{pv,t}^s$ are the wind and PV power curtailment at time t in scenario s, respectively; T denotes the total number of time intervals. $u_{i,t}$ is the operation status of unit i at time t where 1 means online and 0 means offline. $C_{AA-CAES}^{Rp}$ and $C_{AA-CAES}^{Rn}$ are the positive and negative standby market cost, respectively. $C_{AA-CAES}^G$ and $C_{AA-CAES}^C$ are the positive and negative standby market cost, respectively. Shut-down cost of a thermal unit is constant, and the typical value is zero in standard systems. The detailed symbol description, the value of parameters and corresponding constraints can be found in Appendix A and Appendix B.

The detailed modeling of AA-CAES can be found in Ref. [46]. A detailed explanation of the parameters in Equation (1), such as the retail electricity price, the hybrid DR mechanism including the IBDR of EV retailers and the PBDR of EV users, will be given in the next section. UC is a typical mixed-integer nonlinear programming (MINLP) problem [47]. Piecewise linearization is used to approximate the nonlinear constraints in this problem [48].

2.1.2 Hybrid demand response mechanism

This section further considers power-shedding EV retailers who participate in hybrid DR mechanisms. The proposed hybrid DR mechanism comprises two parts. Firstly, TSO offers conditional incentives to EV retailers to mitigate grid load peaks. The incentive amount is positively correlated with the scheduling of electricity demand during peak (or off-peak) hours. Concurrently, EV retailers can optimize their profits by actively participating in this IBDR mechanism. Secondly, EV users respond to the EV retailers by determining their optimal power demand, aiming to maximize their overall welfare, which encompasses electricity bills and the dissatisfaction cost arising from the PBDR. In the proposed hybrid DR mechanism, EV retailers serve a dual role, they not only provide power to EV users but also function as aggregators. The robust pricing strategy of EV retailers and the PBDR mechanism for EV users are economically interconnected, as the electricity price in the EV user's PBDR mechanism is set by the EV retailer as the retail price. Therefore, further analysis is conducted on the lower-level robust pricing strategy concerning the PBDR mechanism for EV users. The objective of the IBDR is to maximize the utility (TDNs) benefit (see Appendix C for a detailed modeling process):

$$\max_{x,y} \sum_{j=1}^{J} \left[\gamma_j w_j - u_j\right] \tag{8}$$

s.t.

$$u_j - \left(K_1 w_j^2 + K_2 w_j - K_2 w_j \theta_j\right) \geq 0, \text{ for } j = 1, \dots, J \tag{9}$$

$$u_j - \left(K_1 w_j^2 + K_2 w_j - K_2 w_j \theta_j\right) \geq u_{j-1} - \left(K_1 w_{j-1}^2 + K_2 w_{j-1} - K_2 w_{j-1} \theta_{j-1}\right), \text{ for } j = 2, \dots, J \tag{10}$$

where, the above equation includes the amount of power reduction (w /MW) and the incentive obtained (u /￥). γ is the "value of power interruptibility". K_1 and K_2 are cost coefficients. θ_j denotes the willingness to curb power for EV retailer j (θ=1 for the most willing retailer and θ=0 for the least willing). In addition, the "individual rationality constraint" (Inequality (9) ensures that each EV retailer's benefit is greater than or equal to zero) and the "incentive compatibility constraint" (Inequality (10) denotes that retailers with higher levels of load cutting receive more compensation than those with lower levels, in order to incentivize retailers to reduce their load levels) are included.

The above model corresponds to the demand management modeling equation for a static single time period (Equations (8)-(10)). Furthermore, for practicality and economic purposes, it is extended to a dynamic multi-time period. The individual rationality and incentive compatibility constraints are further modified, and the optimization operation is minimized from one day to one hour. Finally, the maximum power constraint and DSOs' incentive total budget are added to the model as actual constraints. The final EV retailers' IBDR mathematical model is as follows:

$$\underset{w,u(max)}{C_{Demond}} = \max_{w,u} \sum_{t=1}^{T} \sum_{j=1}^{J} \left[\gamma_{j,t} w_{j,t} - u_{j,t}\right] \tag{11}$$

s.t.

$$\sum_{t=1}^{T} \left[u_{j,t} - \left(K_{1,j} w_{j,t}^2 + K_{2,j} w_{j,t} - K_{2,t} w_{j,t} \theta_j\right)\right] \geq 0, \text{ for } j = 1, \dots, J \tag{12}$$

$$\sum_{t=1}^{T} \left[u_{j,t} - \left(K_{1,j} w_{j,t}^2 + K_{2,j} w_{j,t} - K_{2,t} w_{j,t} \theta_j\right)\right] \geq \sum_{t=1}^{T} \left[u_{j-1,t} - \left(K_{1,j-1} w_{j-1,t}^2 + K_{2,j-1} w_{j-1,t} -\right.\right.$$

$$K_{2,j-1}w_{j-1,t}\theta_{j-1})\Big], \text{ for } j = 2, \ldots J \tag{13}$$

$$\sum_{t=1}^{T} \sum_{j=1}^{J} u_{j,t} \leq UB \tag{14}$$

$$\sum_{t=1}^{T} w_{j,t} \leq CM_j \tag{15}$$

where, UB is the TDNs' total budget and CM_j is the daily limit of interruptible power for EV retailer j; Inequalities (12) and (13) ensure that the total daily power curtailed and incentives by each EV retailer are less than its daily limit of interruptible power and the DSOs' incentive budget, respectively. Regarding the quadratic term of the model, Appendix B.3 provides the method for its approximate treatment under precision constraints.

2.2 The lower level of the proposed strategy

At the lower level of TDNs, two processes are involved: Firstly, the robust electricity price of the EV retailers is optimized based on the PBDR mechanism for EV users, and it is added as a known variable to the upper-level UC in the TSO. Secondly, based on the EV scheduling plan returned from the upper-level TSO, an OPF optimization is carried out on the specific EV charging and discharging locations on the spatial scale at the DSO level.

2.2.1 Robust pricing strategy of electric vehicle retailer

The goal of the robust pricing strategy is to maximize the profits of EV retailers and EV users. It should be noted that the DR of EV users in this part is a PBDR mechanism. Together with the IBDR mechanism introduced in Section 2.1.2, these two DR mechanisms collectively form the hybrid DR mechanism proposed in this study.

(1) Robust pricing strategy process considering market and electric vehicle uncertainties

The decision variables of EV retailers based on the IBDR mechanism of EV users include the retail electricity price and daily electricity purchase amount while satisfying the constraints of the day-ahead market trading rules, retail market pricing constraints, energy balance constraints, etc. Day-ahead decision-making, as the main problem (MP) in this strategy, achieves maximum day-ahead EV retailers' profits by determining the day-ahead electricity purchase and retail electricity price. In this process, the day-ahead market clearing model serves as a boundary condition, describing the mapping relationship between the day-ahead electricity purchase decision and the clearing price. Meanwhile, EVs' PBDR profit function serves as a boundary condition, describing the mapping relationship between retail electricity prices and EVs' energy plans. The detailed modeling of PBDR mechanism can be found in Appendix D.1.2. Real-time decision-making, as a sub-problem (SP), achieves real-time energy adjustment through optimization of energy storage (ES) and real-time electricity purchase and sales volume. The real-time market electricity price curve is determined by prior knowledge and serves as an exogenous variable in the strategy. Finally, this study considers the uncertainty of EVs and establishes a robust optimization strategy, which is solved through column-and-constraint generation (CC&G) [32] to calculate the retail decision-making and profits of both retailers and EVs. The process is shown in Fig. 2.

(2) Modeling and solution of the two-stage robust pricing optimization strategy

The day-ahead and real-time decision models for the robust pricing strategy of EV retailers are thoroughly modeled in Appendix D.1 and Appendix D.2, respectively. The compact form of the robust pricing strategy model is shown in Equation (16) (see Appendix D for a detailed modeling process):

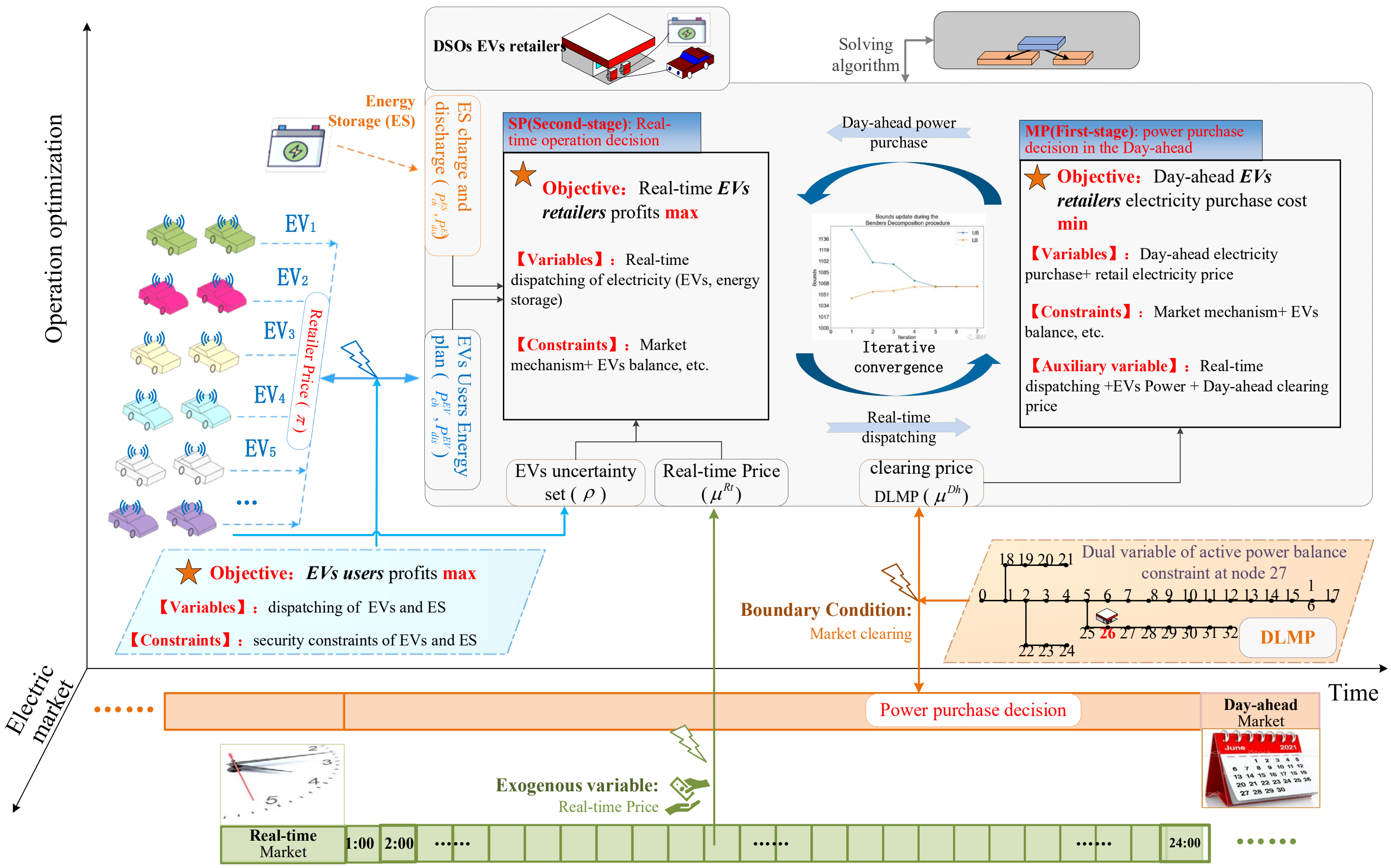

Fig. 2. Process of robust pricing of EV retailers in DSOs.

$$
\begin{cases}
\max\limits_{\{x\in \boldsymbol{X},\boldsymbol{\pi}\in \boldsymbol{\Pi}\}} \boldsymbol{a}^T\boldsymbol{x} + \min\limits_{\{\boldsymbol{\rho}\in\mathcal{R},\boldsymbol{y}_o\in\boldsymbol{Y},\forall o\in\mathcal{O}\}}\max \left(\sum_{o\in\mathcal{O}} v_o \boldsymbol{b}_o^T\boldsymbol{y}_o + N_{EV}\boldsymbol{z}\boldsymbol{\rho}[\boldsymbol{\pi}_{ch}^T - \boldsymbol{\pi}_{dis}^T]\right) \\
\qquad s.t.\ \boldsymbol{A}\boldsymbol{x} + \boldsymbol{B}\boldsymbol{y}_o + \boldsymbol{C}\boldsymbol{z}\boldsymbol{\rho} = \boldsymbol{0},\ \forall o\in\mathcal{O} \\
\max\limits_{z_n=\{p_{ch,n,t}^{EV},p_{dis,n,t}^{EV},\forall t\in T\}} \mathbb{E}(DR_n^{EV}) = \sum_{t\in T_n^{EV}} \left[\sigma_{n,t}^{EV}\left(\varrho_{ch}^{EV}p_{ch,n,t}^{EV} - \frac{p_{dis,n,t}^{EV}}{\varrho_{dis}^{EV}}\right) - \pi_t\left(p_{ch,n,t}^{EV} - p_{dis,n,t}^{EV}\right)\right],\ \forall n\in\mathcal{N}^{EV}
\end{cases}
\tag{16}
$$

where, $\boldsymbol{x}$ and $\boldsymbol{\pi}$ are the decision variables of the first stage, and $\boldsymbol{x} = \{P_{b,t}^{Da}, \forall t\in T\}, \boldsymbol{\pi} = \{\pi_t, \forall t\in T\}$, $\boldsymbol{X}$ and $\boldsymbol{\Pi}$ are its variable space, respectively. $\boldsymbol{y}_o$ is the second stage decision variable corresponding to scenario o, and $\boldsymbol{y}_o = \{P_{b,t,o}^{Re}, P_{s,t,o}^{Re}, P_{ch,t,o}^{ES}, P_{dis,t,o}^{ES}, S_{t,o}^{ES}, \forall t\in T\}$, $\boldsymbol{Y}$ is its variable space. $P_{b,t,o}^{Re}$ and $P_{s,t,o}^{Re}$ refer to the EV retailer's real-time electricity plan under the PBDR of EVs at time t in scenario $\boldsymbol{o}$, respectively. $P_{dis,t,o}^{ES}$ and $P_{dis,t,o}^{ES}$ represent the power schedule of the energy storage system for EV retailer at time t in scenario $\boldsymbol{o}$, respectively. $S_{t,o}^{ES}$ denotes the battery power of the energy storage system at time t in scenario $\boldsymbol{o}$. ϱ_{ch}^{EV} and ϱ_{dis}^{EV} denote the charging and discharging efficiencies of EVs, respectively. $\sigma_{n,t}^{EV}$ represents the unit utility of EV_n at time t. $\boldsymbol{\rho}$ is a vector representing the distribution of uncertain variables, i.e., $\boldsymbol{\rho} = \{\rho_n, \forall n\in\mathcal{N}_*^{EV}\}$, where it signifies the proportion of each type of EV. $\boldsymbol{\rho}_0$ is the empirical distribution of uncertain variables obtained through clustering, indicating the frequency of each type of EVs in historical data. $\mathcal{O}$ is a real-time DLMP scene set, v_o represents the occurrence probability of scenario o, z_n denotes the charging and discharging schedule for EV_n, i.e., $z_n = \{p_{ch,n,t}^{EV}, p_{dis,n,t}^{EV}, \forall t\in\mathcal{T}\}$, with $\boldsymbol{Z}_n$ as its variable space, as defined in Appendix D. $p_{ch,n,t}^{EV}$ and $p_{dis,n,t}^{EV}$ represent the charging and discharging schedule for EV_n. $\boldsymbol{z}$ is a row vector representing the aggregate energy plan for different types of EVs, i.e., $\boldsymbol{z}=[\boldsymbol{z}_1 \quad \boldsymbol{z}_2 \quad \cdots \quad \boldsymbol{z}_n], \forall n \in \mathcal{N}_*^{\mathrm{EV}}$. $\boldsymbol{a}$、$\boldsymbol{A}$、$\boldsymbol{B}$ and $\boldsymbol{C}$ are coefficient vectors and matrices, b_o is the coefficient vector corresponding to scenario o. $\boldsymbol{c}_n$ is the coefficient vector corresponding to EV_n. $\mathbb{E}\{\cdot\}$ denotes the expected value of EV users' profits, which indicates the PBDR mechanism of EV users. As a follower, the PBDR, along with the main robust optimization problem, forms a Stackelberg model.

The above model constitutes a multi-stage, multi-layer planning, which cannot be directly solved. Therefore, this paper decomposes it into a robust optimization MP and SP, employing the CC&G algorithm for iterative resolution. The definition of the robust optimization MP is provided in Appendix D.1, with its physical interpretation being: under a given combination of EVs, the EV retailer optimizes day-ahead purchased electricity quantity and retail prices to maximize its own revenue. The definition of the robust optimization SP is detailed in Appendix D.2, with its physical interpretation being: under known day-ahead electricity purchase contracts and retail prices, considering the real-time optimization scheduling of the energy management system, find the worst-case combination of EVs. Based on the detailed simplification processes in Appendix D.1 and Appendix D.2 for the robust optimization MP and SP, the robust optimization MP at the k-$_{th}$ iteration is transformed into the mixed-integer quadratic programming (MIQP), as illustrated in Equation (17) (see Appendix D.1 for a comprehensive modeling process).

$$\begin{gathered}
\max_{\{F,\boldsymbol{x}\in\boldsymbol{X},\boldsymbol{\pi}\in\boldsymbol{\Pi},\boldsymbol{y}_{o,k}\in\boldsymbol{Y},\forall o\in\mathcal{O},\forall k\in\mathcal{K},\forall n\in\mathcal{N}_*^{\mathrm{EV}},z_s\in Z_a,\zeta_e\}} (a^{\mathrm{T}}\boldsymbol{x}+F) \\
\text{s.t. } F \le N_{\mathrm{EV}}\boldsymbol{\beta}\boldsymbol{\rho}_{k^*} + \textstyle\sum_{o\in\mathcal{O}} v_o \boldsymbol{b}_o^T \boldsymbol{y}_{o,k}, \forall k\in\mathcal{K} \\
\boldsymbol{x}+\boldsymbol{B}\boldsymbol{y}_{o,k}+\boldsymbol{C}z\boldsymbol{\rho}_{k^*}=\boldsymbol{0}, \forall o\in\mathcal{O}, \forall k\in\mathcal{K} \\
[\boldsymbol{\pi}_{ch}^T-\boldsymbol{\pi}_{dis}^T]-\boldsymbol{\zeta}_n^{\mathrm{T}}\boldsymbol{E}_n-\boldsymbol{c}_n^{\mathrm{T}}=\boldsymbol{0}, \forall n\in\mathcal{N}_*^{\mathrm{EV}} \\
(\boldsymbol{E}_n z_n-\boldsymbol{e}_n)\perp\boldsymbol{\zeta}_n\ge\boldsymbol{0}, \forall n\in\mathcal{N}_*^{\mathrm{EV}}
\end{gathered} \tag{17}$$

where, $\boldsymbol{\rho}_{k^*}$ represents the worst-case EVs set returned by the sub-problem at the k-$_{th}$ iteration, given as a parameter in the master problem; $\boldsymbol{y}_{o,k}$ is the newly introduced variable associated with $\boldsymbol{\rho}_{k^*}$, serving as a decision variable in the MP; $\mathcal{K}$ denotes the iteration set; F is an auxiliary variable introduced to connect the main and sub-problems of the CC&G. $\boldsymbol{E}_n$ and $\boldsymbol{e}_n$ are coefficient matrix and vector of EV_n, respectively. ζ_n is the dual variable. $\boldsymbol{\zeta}_n$ is the dual variable. F is an auxiliary variable introduced. The symbol "$\perp$" denotes the complementary slackness condition. $\boldsymbol{\beta}$ represents a row vector constituting the energy cost of different types of EVs, namely $\boldsymbol{\beta}=[\zeta_n^{\mathrm{T}}\boldsymbol{e}_n+\boldsymbol{c}_n^{\mathrm{T}}z_n, \forall n\in\mathcal{N}_*^{\mathrm{EV}}]$.

The robust optimization SP at the k-$_{th}$ iteration is converted into a mixed-integer programming problem, as illustrated in Equation (18) (see Appendix D.2 for a detailed modeling process).

$$\begin{gathered}
\min_{\boldsymbol{\rho}\in\boldsymbol{\mathcal{R}},\{\boldsymbol{y}_o\in\boldsymbol{Y},\boldsymbol{\mu}_o,\omega_o,\forall o\in\mathcal{O}\}} \left(N_{\mathrm{EV}}[\boldsymbol{\pi}_{ch,k^*}^{\mathrm{T}}-\boldsymbol{\pi}_{dis,k^*}^{\mathrm{T}}]\boldsymbol{z}_{k^*}\boldsymbol{\rho}+\textstyle\sum_{o\in\mathcal{O}} v_o\boldsymbol{b}_o^T\boldsymbol{y}_o\right) \\
\text{s.t.}\begin{cases}
\boldsymbol{A}x_{k^*}+\boldsymbol{B}y_o+\boldsymbol{C}z_{k^*}\boldsymbol{\rho}=0, \forall o\in\mathcal{O} \\
\boldsymbol{v}_o\boldsymbol{b}_o^T-\boldsymbol{\partial}_o^T\boldsymbol{B}-\mathcal{E}_o^T\boldsymbol{M}=0, \forall o\in\mathcal{O} \\
(\boldsymbol{M}y_o-\boldsymbol{m})\perp\mathcal{E}_o\ge 0, \forall o\in\mathcal{O}
\end{cases}
\end{gathered} \tag{18}$$

where, $\boldsymbol{x}_{k^*}$ denotes the numerical value of purchased electricity quantity at the k-$_{th}$ iteration; $\boldsymbol{\pi}_{ch,k^*}^T$ and $\boldsymbol{\pi}_{dis,k^*}^T$ represent the value of the charging and discharging retail price during the k-$_{th}$ iteration, respectively. $\boldsymbol{z}_{k^*}$ suggests the charging and discharging quantity of EVs at the k-$_{th}$ iteration. Given $\boldsymbol{\pi}_{k^*}$, the values of $\boldsymbol{z}_{k^*}$ can be calculated using the EV users' demand response model (Appendix D.1.2). $\boldsymbol{\partial}_o$ and $\mathcal{E}_o$ are dual variables. $\boldsymbol{M}$ and $\boldsymbol{m}$ are coefficient matrix and vector of EV_n, respectively.

The original objective functions, constraints, and decision variables of each stage are shown in Appendix D. The Pseudocode for solving the two-stage robust pricing model by CC&G is shown in Algorithm 1.

ALGORITHM1: TWO-STAGE ROBUST OPTIMIZATION SOLUTION STRATEGY BASED ON CC&G

Input: *Real-time DLMP; EVs:* $N_{EV}+N_{type}$ *; Empirical distribution* $\boldsymbol{\rho_0}$ *;*

Output: *Day-ahead power purchase cost and expected benefits of real-time (RT); retail electricity price* $\boldsymbol{\pi}_k$

1 *Objective function* $\leftarrow \max_{\boldsymbol{x},\boldsymbol{\pi}} \boldsymbol{a}^T\boldsymbol{x} + \min_{\{\boldsymbol{\rho}\in\boldsymbol{\mathcal{R}},\boldsymbol{y}_o\in\boldsymbol{Y},\forall o\in\mathcal{O}\}}\max \left(N_{EV}\boldsymbol{z}\boldsymbol{\rho}[\boldsymbol{\pi}_{ch}^T-\boldsymbol{\pi}_{dis}^T]+\sum_{o\in\mathcal{O}} v_o\boldsymbol{b}_o^T\boldsymbol{y}_o\right)$

2 ***Initialization of variables: LB***$\leftarrow$*-∞ ;* ***UB***$\leftarrow$*+∞ ; k*$\leftarrow$*1;* $\boldsymbol{\mathcal{O}}\leftarrow\emptyset$*;*

3 ***Solve*** *the following master problem* ***MP*** *by* ***Gurobi****:*

$$\textbf{\textit{MP (MILP):}}\ \max_{\left\{\substack{F,\boldsymbol{x}\in\boldsymbol{X},\boldsymbol{\pi}\in\boldsymbol{\Pi},\boldsymbol{y}_o^{k*}\in\boldsymbol{Y},\forall o\in\mathcal{O},\\ \forall k\in\mathcal{K},\forall n\in\mathcal{N}_*^{EV},z_n\in Z_n,\boldsymbol{\zeta}_n}\right\}}(\boldsymbol{a}^T\boldsymbol{x}+F);\ s.t.\begin{cases} F\le N_{EV}\boldsymbol{\beta}\boldsymbol{\rho}_{k^*}+\sum_{o\in\mathcal{O}}v_o\boldsymbol{b}_o^T\boldsymbol{y}_o^{k*}\\ \boldsymbol{Ax}+\boldsymbol{By}_o^{k*}+\boldsymbol{C}z\boldsymbol{\rho}_{k^*}=\boldsymbol{0}\\ [\boldsymbol{\pi}_{ch}^T-\boldsymbol{\pi}_{dis}^T]-\boldsymbol{\zeta}_n^T\boldsymbol{E}_n-\boldsymbol{c}_n^T=\boldsymbol{0}\\ (\boldsymbol{E}_n z_n-\boldsymbol{e}_n)\perp\boldsymbol{\zeta}_n\ge\boldsymbol{0}\end{cases},\forall o\in\mathcal{O},\forall n\in\mathcal{N}_*^{EV},\forall k\in\mathcal{K};$$

- Output Day-ahead purchased Power $\boldsymbol{x}_{k+1^*}$*; Retail electricity price* $\boldsymbol{\pi}_{k+1^*}$*; Derive an optimal solution* $(\boldsymbol{x}_{k+1}^*,F_{k+1}^*,\boldsymbol{y}_o^{1*},\dots,\boldsymbol{y}_o^{k*})$*, and update* $\boldsymbol{LB}=max\{\boldsymbol{LB},\boldsymbol{a}^T\boldsymbol{x}_{k+1}^*+\boldsymbol{F}_{k+1}^*\}$

4 ***Solve*** *the following sub-problem* ***SP*** *by* ***Gurobi****:*

$$\textbf{\textit{SP(MILP):}}\ \mathcal{Q}(\boldsymbol{x}_{k+1}^*)=\min_{\left\{\substack{\boldsymbol{\rho}\in\boldsymbol{\mathcal{R}},\boldsymbol{y}_o\in\boldsymbol{Y},\\ \boldsymbol{\partial}_o,\mathcal{E}_o,\forall o\in\mathcal{O}}\right\}}\left(N_{EV}\boldsymbol{z}_{k^*}\boldsymbol{\rho}[\boldsymbol{\pi}_{ch,k^*}^T-\boldsymbol{\pi}_{dis,k^*}^T]+\sum_{o\in\mathcal{O}} v_o\boldsymbol{b}_o^T\boldsymbol{y}_o\right);\ s.t.\begin{cases}\boldsymbol{Ax}_{k^*}+\boldsymbol{By}_o+\boldsymbol{Cz}_{k^*}\boldsymbol{\rho}=\boldsymbol{0}\\ v_o\boldsymbol{b}_o^T-\boldsymbol{\partial}_o^T\boldsymbol{B}-\mathcal{E}_o^T\boldsymbol{M}=\boldsymbol{0}\\ (\boldsymbol{My}_o-\boldsymbol{m})\perp\mathcal{E}_o\ge\boldsymbol{0}\end{cases},\forall o\in\mathcal{O};$$

- Calculation of $\boldsymbol{z}_{n,k^*}$ *based on EV(n) demand response model and* $\boldsymbol{z}_{k^*}$*;*

-Output Worst-case distribution $\boldsymbol{\rho}_{k^*}$*; Retail electricity price* $\boldsymbol{\pi}_{k^*}$*; and update* $\boldsymbol{UB}=min\{\boldsymbol{UB},\boldsymbol{a}^T\boldsymbol{x}_{k+1}^*+\mathcal{Q}(\boldsymbol{x}_{k+1}^*)\}$

5 ***if*** $UB-LB\le\epsilon$*, return* $\boldsymbol{x}_{k+1^*}$*,* $\boldsymbol{\pi}_{k+1^*}$*; and terminate. Otherwise, do*

6 ***if*** $\mathcal{Q}(\boldsymbol{x}_{k+1}^*)<+\infty$

return $\boldsymbol{\rho}_{k+1^*}$*, create variable* $\boldsymbol{y}_o^{k+1}$ *and add the following constraint:*

7 $F\le N_{EV}\boldsymbol{z}_{k^*}\boldsymbol{\rho}[\boldsymbol{\pi}_{ch,k^*}^T-\boldsymbol{\pi}_{dis,k^*}^T]+\sum_{o\in\mathcal{O}} v_o\boldsymbol{b}_o^T\boldsymbol{y}_o^{k+1};\ \boldsymbol{Ax}_{k+1^*}+\boldsymbol{By}_o^{k+1}+\boldsymbol{Cz}_{k+1^*}\boldsymbol{\rho}=\boldsymbol{0},\forall o\in\mathcal{O}$

to ***MP*** *where* $\boldsymbol{\pi}_{k+1^*}$*,* $\boldsymbol{z}_{k+1^*}$ *is the optimal scenario solving* $\mathcal{Q}(\boldsymbol{x}_{k+1}^*)$*.*

8 *update* $k=k+1,\boldsymbol{O}=\boldsymbol{O}\cup\{k+1\}$ *and go to step 3.*

9 ***if*** $\mathcal{Q}(\boldsymbol{x}_{k+1}^*)=+\infty$

return $\boldsymbol{\rho}_{k+1^*}$*, create variable* $\boldsymbol{y}_o^{k+1}$ *and add the following constraint:*

10 $$\boldsymbol{Ax}_{k+1^*}+\boldsymbol{By}_o^{k+1}+\boldsymbol{Cz}_{k+1^*}\boldsymbol{\rho}=\boldsymbol{0},\forall o\in\mathcal{O}$$

to ***MP*** *where* $\boldsymbol{\pi}_{k+1^*}$*,* $\boldsymbol{z}_{k+1^*}$ *is the identified scenario for which* $\mathcal{Q}(\boldsymbol{x}_{k+1}^*)=+\infty$

11 *update* $k=k+1$ *and go to step 3.*

12 ***end***

Notes: The variable $\boldsymbol{\rho}_{k+1^*}$ represents the worst combination of EVs returned by the subproblem at the k-$_{th}$ iteration, which is a given parameter in the MP. The variable $\boldsymbol{y}_{o,k+1}$ is the new variable introduced corresponding to $\boldsymbol{\rho}_{k+1^*}$ and is a decision variable in the MP.

2.2.2 Optimal strategy for optimal power flow

According to the optimization results obtained from the upper-level (i.e., EV charging and discharging plan), the goal of the lower-level distribution network is to minimize network losses and voltage deviation by arranging EVs to charge and discharge at the optimal positions of the radial distribution network. This can be viewed as a typical OPF problem. To simplify the simulation of the behavioral distribution of EVs, the distribution network is divided into three areas: residential areas, commercial areas, and official areas [34]. The slack node of the bus is equivalent to an infinite system (corresponding to TSO), which is used to provide electrical energy. The objective of the OPF is:

$$min\, E(\sum_{t=1}^{T} [\sum_{pq\epsilon\phi}(I_{pq,t}^{2} r_{pq}) + \sum_{n=1}^{N_{branch}} (U_{p,t} - U_{ref})^{2}]) \tag{19}$$

where, $E\{\cdot\}$ denotes the mathematical expectation of all scenarios. pq represents the branch connecting nodes p and q in DSOs. Φ is the set of branches in DSOs. r_{pq} is the resistance of branch pq. T is the total number of time periods in one day. $I_{pq,t}$ denotes the current flowing through branch pq at time t. $U_{p,t}$ represents the voltage of node p at time t. N_{branch} refers to the number of distribution network branches. U_{ref} is the expected voltage of nodes. Scenarios are the same to the upper layer. The corresponding constraints can be found in Appendix E. Currently, OPF has been proven to be an NP-hard and non-convex optimization problem [49]. The convex relaxation [50, 51] can transform the OPF into a mixed-integer second-order cone programming (MISOCP) problem that can be accurately solved by GUROBI [52]. Appendix F provides a detailed explanation.

3 Case study

The effectiveness of the proposed bi-level optimization strategy for large-scale EVs in TDNs is verified by an integrated model of TDNs. As shown in Fig. 1(b), the distributed network is simulated using the IEEE 33 distribution network [53] with the robust pricing strategy and hybrid DR mechanisms, as well as a transmission grid that includes a 110 MW wind farm, a 170 MW PV system, an AA-CAES device, and 10 conventional thermal power units. Scenarios of wind power and their probability data are collected from [54]. Solar power output data is collected from [55], and wind and solar outputs are matched to the total installed capacity using certain scaling factors. The maximum charging and discharging power of AA-CAES energy storage, the electricity prices in positive and negative reserve markets, and daily prices are referred to in [56]. The economic mechanisms for DSO, EV retailers, and EV users can be found in [57]. The total number of EVs that can participate in scheduling in the transmission network coverage area is set at 150,000, with an average charging and discharging power of 1.8 kW. The scheduling frequency is once per day. It is assumed that there is one similarly configured EV retailer at each distribution network within the coverage area of the transmission network [58]. In each distribution network, the distribution of EVs in the three areas is 70%, 20%, and 10%, respectively. In addition, 80% of the cars in residential areas commute to office areas, and 15% commute to commercial areas. Other detail parameters can be found in Appendix A and Appendix G.

3.1 Case study and simulation data

In order to evaluate the performance of the proposed strategy, ten tests are considered in this work. To assess the practicability of the robust pricing strategy, explore the impact of the hybrid DR mechanisms on the operation of the TDNs, and understand the influence of various electricity price profiles and EV penetrations on the upper layer UC optimization result of TSO, Tests 1-6 were examined in the UC optimization problem. To derive more universally applicable conclusions about the hybrid DR mechanism, a sensitivity analysis is conducted on the key parameters of the IBDR mechanism for EV retailers and the PBDR mechanism for EV users in Test 7. Additionally, to demonstrate the generalizability and robustness of the robust pricing strategy for EV retailers, in Test 8, this paper considers the empirical distribution obtained by clustering as the true distribution and uses it as a control experiment. Based on the scheduling plans for large-scale EVs by upper-level TSO's optimization in the time domain, the lower-level DSO further optimizes the optimal charging and discharging locations for EVs in the spatial domain. The coefficients of the base load curve in the distribution network are identical to those used in the transmission system. In the distribution network, Tests 9 and 10 are added to verify the advantages of the lower-level optimization model.

Test 1: EVs are not considered in the TDNs system.

Test 2: There are 150,000 EVs in the system, and the charging and discharging prices are constant and equal throughout the day.

Test 3: There are 150,000 EVs in the system, and the charging and discharging prices fluctuate with the load (appearing as a bimodal distribution).

Test 4: There are 150,000 EVs in the system, and the charging and discharging retail prices are determined based on robust pricing in this article (appearing as a unimodal distribution, a control experiment with Test 3).

Test 5: There are 100,000 EVs in the system, and the price curve is the same as Test 4.

Test 6: There are 50,000 EVs in the system, and the price curve is the same as Test 4.

Test 7: The sensitivity analysis of the hybrid DR mechanism, including the IBDR mechanism of EV retailers and the PBDR mechanism of EV users.

Test 8: The robust analysis of the robust retail electricity pricing strategy.

Test 9: Simulate without considering EVs under the same conditions as Test 1.

Test 10: Simulate the same conditions as Test 4, with the distribution of EVs in the three areas shown in Fig. 1(b).

Table 2. Varying parameters for different EV retailers.

EV retailers	$K_{1,j}$	$K_{2,j}$	θ_j	CM_1(MWh)	CM_2(MWh)	CM_3(MWh)	CM_4(MWh)	CM_5(MWh)
1	1.847	11.64	0	160	170	180	190	200
2	1.378	11.63	0.14	210	230	230	240	250
3	1.079	11.32	0.26	290	300	310	320	330
4	0.9124	11.5	0.37	370	380	390	400	410
5	0.8794	11.21	0.55	420	430	440	450	460
6	1.378	11.63	0.84	510	520	530	540	550
7	1.5231	11.5	1	580	590	600	610	620
Total	-	-	-	2540	2620	2680	2750	2820

In the above ten tests, for ease of analysis, some of the model parameters of EV retailers and EV users are simplified in this article. As shown in Table 2, it is assumed that TDNs operators know each EV retailer's daily limit of interruptible energy (CM_j), the willingness (θ_j) to curb electric power, the outage cost function coefficients of participating retailers ($K_{i,j}$), and their daily DR cost budget (UB) is \$ 150, 000. As shown in Fig. 3, assuming that the γ values of EV retailer 1, EV retailer 2, and EV retailer 3 are 120%, 115%, and 105% of their initial values, while the γ values of EV retailer 5, EV retailer 6, and EV retailer 7 are 90%, 83%, and 75% of their initial values [54].

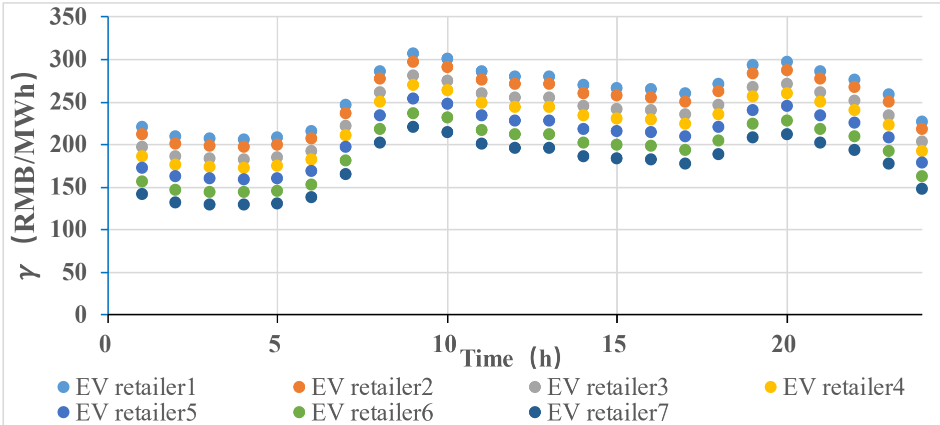

Fig. 3. Varying values of γ.

The EV retailers are equipped with energy storage devices. After proportional scaling, the EV retailer possesses an energy storage system with a capacity of 1000 kWh, and both its maximum charging and discharging power are set at 250 kW. The EV retailer's average daily service capacity for EVs has been reduced to 60 following a proportional scaling principle. The EV retailer connects to the distribution network through electrical node 26, with a maximum day-ahead purchase of 500 kWh and a maximum real-time purchase or sale of 500 kWh. The pricing between EV retailers and the power grid is determined based on the DLMP, which is provided in Appendix G. The upper and lower limits of the retail electricity price are set at 80% and 120% of the DLMP, respectively. To further address the uncertainty in real-time electricity market prices, this work applies the combination of Elbow and K-Means Methods clustering algorithm to 1000 historical real-time electricity price data points for a specific EV charging station. Based on the combination of elbow method and K-Means clustering algorithm, the historical dataset is ultimately grouped into 10 distinct clusters. The comprehensive clustering process is described in Appendix A.3. All calculations were performed on a computer with an Intel (R) Core (TM) i7-2500 3.9 GHz CPU, 8 GB of RAM, the Windows 11 operating system, and the GUROBI 10.0 optimization platform. The simulation was conducted over a 24-hour period.

3.2 Upper level: transmission network

At the upper transmission grid level, the UC optimization coordinates the scheduling of the hybrid DR power of large-scale EVs and TDNs based on the robust pricing strategy of EV retailers. The optimized results of the overall upper-level UC optimization results of the entire TDNs, the robust pricing strategy for EV retailers, the analysis of the PBDR mechanism for EV users, and the sensitivity analysis of the IBDR mechanism for EV retailers are all discussed in this section (Tests 1-7).

3.2.1 Optimal results of the unit commitment

The scheduling price profiles of Tests 1-6 can be observed in Fig. 4. The objective function, EV charging cost, EV retailer IBDR cost, AA-CAES operating cost, fuel cost, PM2.5 emission cost, start-up cost, and corresponding expected curtailment of renewable energy under Tests 1-6 are shown in Table 3. It can be seen that the total objective function value decreases from Test 4 to Test 6 and then to Test 1 (as the number of EVs decreases), the charging costs of EV users decrease, and the IBDR costs increase (equivalent revenue decreases). Since the total capacity of renewable energy is relatively small compared to that of thermal power units, the power system can achieve 100% renewable energy consumption efficiency. These results are in line with the optimized operation of the electricity market.

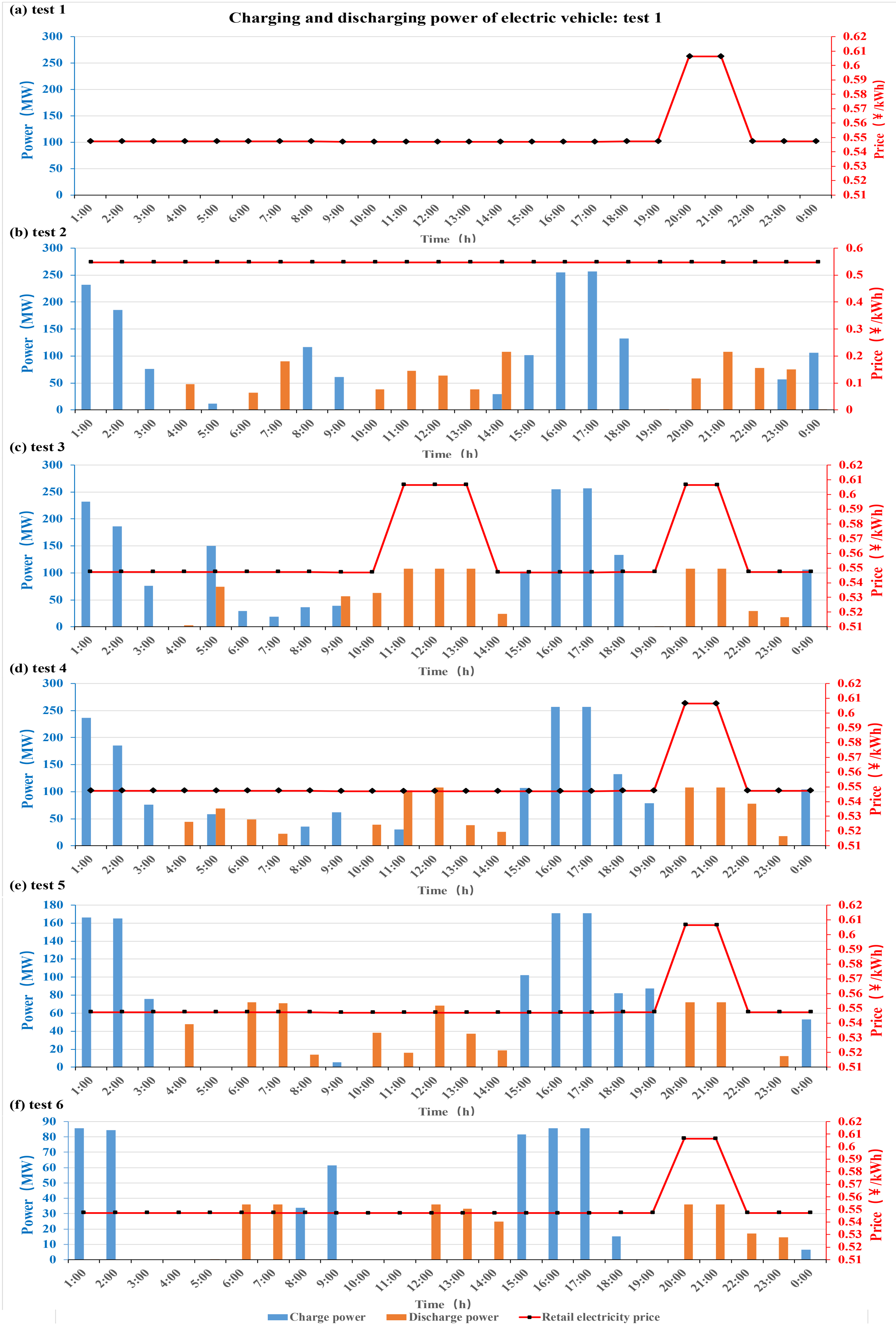

Fig. 4. The retail electricity price and EVs charging/discharging results of different tests.

Fig. 5. The UC results of different tests.

Table 3. The value of objective function in different cases.

Test	Objective function (￥)	Fuel cost (￥)	Start-up cost (￥)	Emission cost (￥)	Charging cost (￥)	AA-CAES (￥) Purchase cost	AA-CAES (￥) Reserve market	Demand response(￥)	Abandon Wind/PV (MW)
1	1544862	431230	19126	89039	0	-281400	769921	526946	0
2	1991267	436536	14035	91623	443319	-281400	769538	517615	0
3	1959863	437306	14448	91676	411230	-281400	769500	517103	0
4	1972420	435939	15204	91694	430414	-281400	770714	509854	0
5	1843970	433363	25868	90821	286964	-281400	773067	515286	0
6	1691540	432896	16030	89945	143442	-281400	769500	521127	0

The results of the charging and discharging dispatch plan under Tests 1-6 are shown in Figs. 4 and 5. The difference between the load curve after considering the hybrid DR mechanism and the total output of each unit in the transmission network is regarded as the load of EVs. The analysis of the results is as follows:

The impact of different EV penetration rates on UC results in Tests 1, 4, 5, and 6 is compared. As shown in Table 3, the operating cost of the power system increases with the increase in EV penetration rate as more power is provided for EVs. The overall installed output curve becomes smoother, which means that the peak load is compensated by EVs load affected by more price changes (like the IBDR mechanism of EV retailers in Section 2.1.2).

The impact of different price curves on the charging and discharging plans of EVs in Tests 2, 3, and 4 is compared. In Test 2, EVs are charged and discharged at the same constant price, so the optimal target is only related to the optimized operation of the power system, and the charging and discharging of EVs are more chaotic and disordered. In Tests 3 and 4, EVs will use the "peak-valley difference arbitrage" concept to charge at low prices and discharge at high prices. Although the operating cost of Test 2 is the lowest, it is difficult to meet the corresponding EV charging and discharging loads during the peak period of commuting in reality. In contrast, under the price scenario of Tests 3 and 4, users will charge and discharge during the off-peak period, which is more effective and practical at the TDNs level. The solution to Tests 3 and 4 is the same, only the charging and discharging price trends are different. Compared with Test 2, due to price fluctuations, the charging and discharging interval ranges of Tests 3 and 4 are more concentrated.

In the UC optimization model, the following parameters were further collected: the total EV retailers' incentive (i.e., the total amount of currency received by EV retailers per day as the incentive for participating in IBDR) and the total energy reduced by retailers (i.e., the total energy reduced by EV retailers within 24 hours). Considering the user goals of large-scale EVs and from the perspective of the long-term operation of TDNs, the robust pricing strategy of Test 4, the proposed robust pricing strategy in this work, is the best way to optimize large-scale EVs in TDNs uniformly. A detailed and comprehensive analysis of the robust pricing strategy of EV retailers and the hybrid DR mechanisms of EVs will be given in the next two sections.

3.2.2 Analysis of hybrid demand response mechanism

To further analyze the robustness and rationality of the IBDR mechanism between EV retailers and TDNs, which is the second part of the proposed hybrid DR mechanism, the section continues its examination from the DR perspective on Tests 1-6 discussed in Section 3.2.1 and analyzes the results of Test 7.

(1) Analysis of the incentive-based demand response mechanism

Fig. 6 shows the load operation curve of Tests 1-6 in Section 3.2.1 after IBDR. It is not difficult to find that the IBDR mechanism of EV retailers can significantly reduce the peak value of the original load curve, increase the low valley of the original load curve, and ultimately achieve uniform distribution of the load (similar to peak shaving and valley filling). As for Test 7, the total energy reduced by each EV retailer within 24 hours, as well as the corresponding optimal incentive received by each retailer, are shown in Table 4. Table G.1 in Appendix G shows the γ values for different EV retailers, and the impact on the results for TDNs as well as EV retailers can be observed from Table 4. It is not difficult to find a relationship between γ and retailers: retailers with reduced γ receive less incentive for reducing the same power, while EV retailers with increased γ receive more incentive. It is worth noting that the incentive compatibility constraint in the Stackelberg game remains unchanged and is not violated.

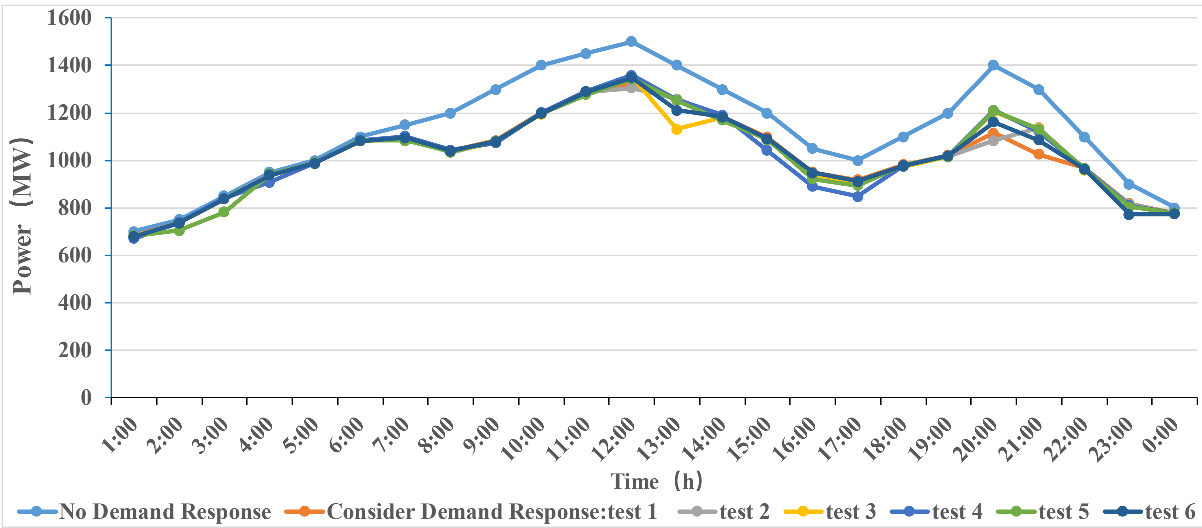

Fig. 6. Load demand with EV retailers' DR considered or not.

Table 4. Total energy curtailed and EV retailers' incentive received.

EV retailers	Energy saved (MWh)	Incentive received (￥)
1	180	59958.08988
2	230	55884.53712
3	310	80128.1763
4	390	80915.0661
5	440	92539.1061
6	530	172554.1335
7	600	180535.2873
Total	2680	722514.3276

(2) Analysis of the price-based demand response mechanism

As shown in Fig. 7, the results show that the charging and discharging of EVs occurred during low electricity demand periods and high electricity demand periods, respectively, and EVs can be regarded as movable and flexible energy storage devices. This indicates that the proposed PBDR mechanism in the hybrid DR mechanism enables the effective participation of EV users in electricity management, leading to tangible benefits for them. Besides, the real-time electricity purchase and sale by EV retailers followed a profit-making pattern of buying electricity during low-price periods and selling during high-price periods. Energy storage serves as a flexible unit for power retailers, and its charging and discharging status is consistent with that of EV retailers. The real-time buying and selling curves of the retailers under the other 9 different real-time DLMP curve scenarios (Fig. A.3, in Appendix A) have some differences, but all follow the rule of "charging during low electricity demand periods and discharging during high electricity demand periods", which indicates the effectiveness of the PBDR of EV users. On the other hand, the flexibility of energy storage systems expands the decision space of the energy management system, enabling the EV retailer to mitigate the adverse effects caused by the uncertainty in the electricity consumption of EV users.

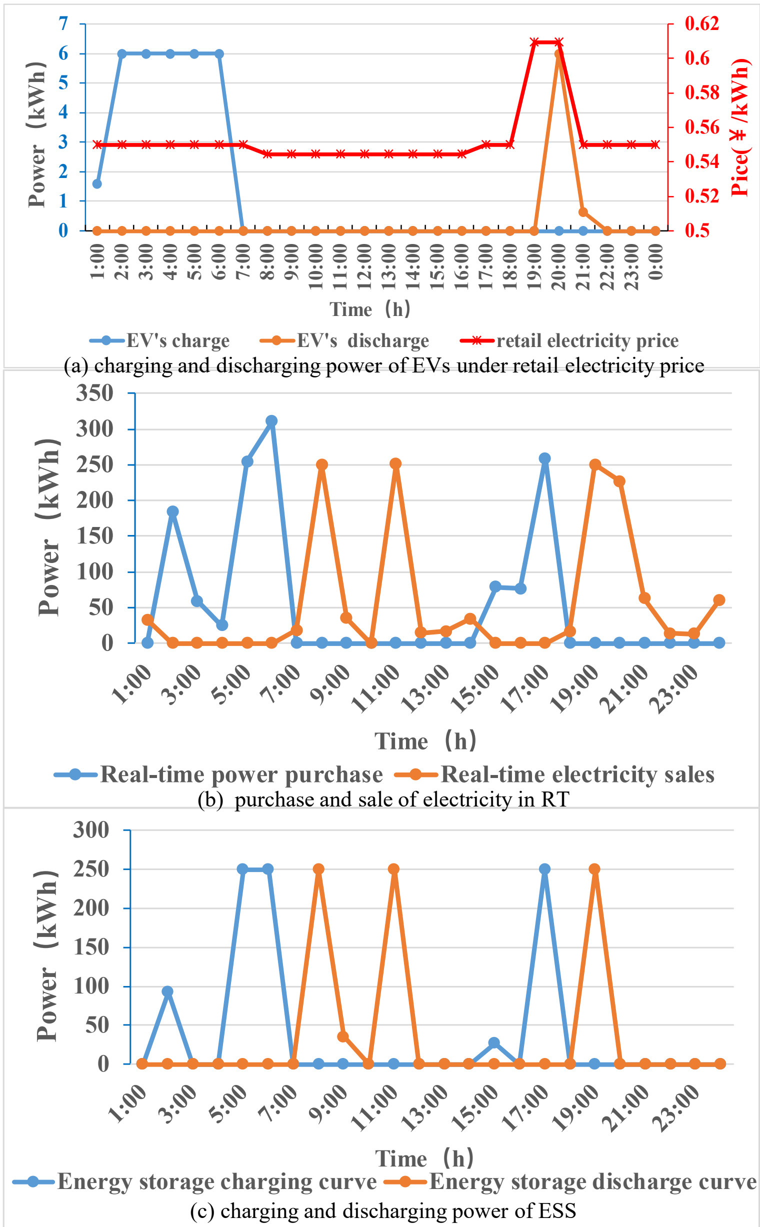

(a) charging and discharging power of EVs under retail electricity price
(b) purchase and sale of electricity in RT
(c) charging and discharging power of ESS

Fig. 7. Curve of power in Real-time (p=0.105, category 1).

3.3 Lower level: distribution network

The robust pricing of EV retailers and the upper-level UC optimization for TSO are conducted as parallel optimizations. Test 8 is set to analyze the robustness of the robust retail electricity pricing strategy for EV retailers. Based on the load periods of EVs in the time domain, which are calculated from the upper-level UC problem, to mainly analyze the impact of different EV load locations and different penetrations of EVs on the distribution network optimization, Tests 9-10 are mainly investigated in the lower-level OPF optimization program.

3.3.1 Robust analysis for pricing strategy

The iterative solution process of the CC&G algorithm for the two-stage robust optimization of the retail electricity price is presented in Fig. 8. As the iterations of the MP and SP proceed, the upper and lower bounds approach each other, and convergence is achieved after three iterations, which ensures the timeliness and applicability of the pricing strategy. The pricing curves and revenue under the determined distribution and worst-case distribution from robust optimization are shown in Fig. 9, respectively. The results show that the proposed robust pricing strategy can effectively reduce the fluctuation range of EV retailers' revenue while maintaining a higher average revenue compared to the deterministic optimization strategy. This indicates that the proposed robust optimization strategy fully considers the deviation between the actual distribution and empirical distribution, broadens the search range of the retailer's strategy, and is more universally applicable. From a long-term operational perspective, the results obtained from robust optimization can adapt to more practical scenarios and improve EV retailers' expected revenue.

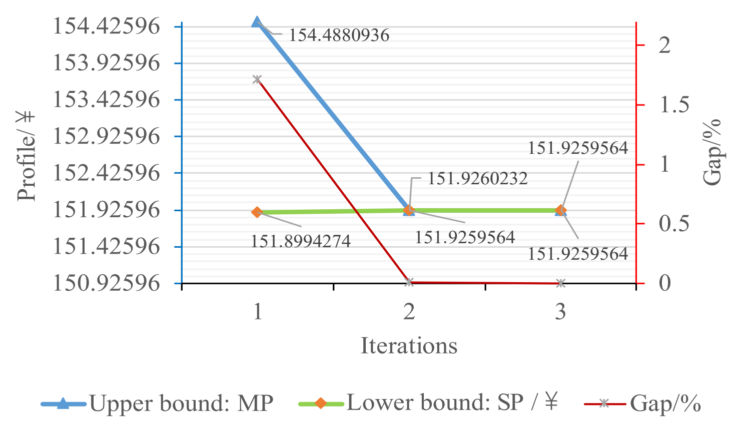

Fig. 8. Iterative results of CC&G.

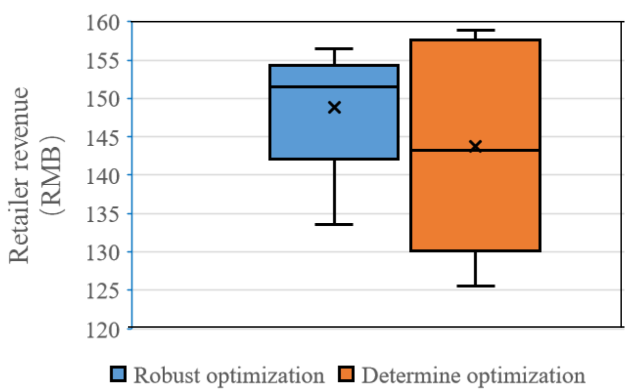

Fig. 9. Boxplot of benefit in different pricing strategies.

3.3.2 Optimal results of the optimal power flow

The charging and discharging scheduling results of EVs in Test 10 are shown in Figs. 10 (a)-(b), respectively. The spatial distribution of EV charging and discharging loads in the network is shown in Fig. 11 (c). It can be seen that the charging load is mainly concentrated at nodes 1, 5, 6, 11, 12, 13, 18, 19, 20, 21, 31, and 32, while the discharging load is mainly concentrated at nodes 4, 15, 16, 17, 24, and 30. It is not difficult to observe that the charging load of EVs is arranged near the slack bus, while the discharging load is arranged near the end node. This is because the power flow of the radial distribution network flows from the source node to the end node, and most of the power is provided by the slack bus node (equivalent to TSO), which can reduce network losses. The time distribution of charging and discharging of the lower-level EVs is completely consistent with that of the upper-level transmission network as flexible energy storage units.

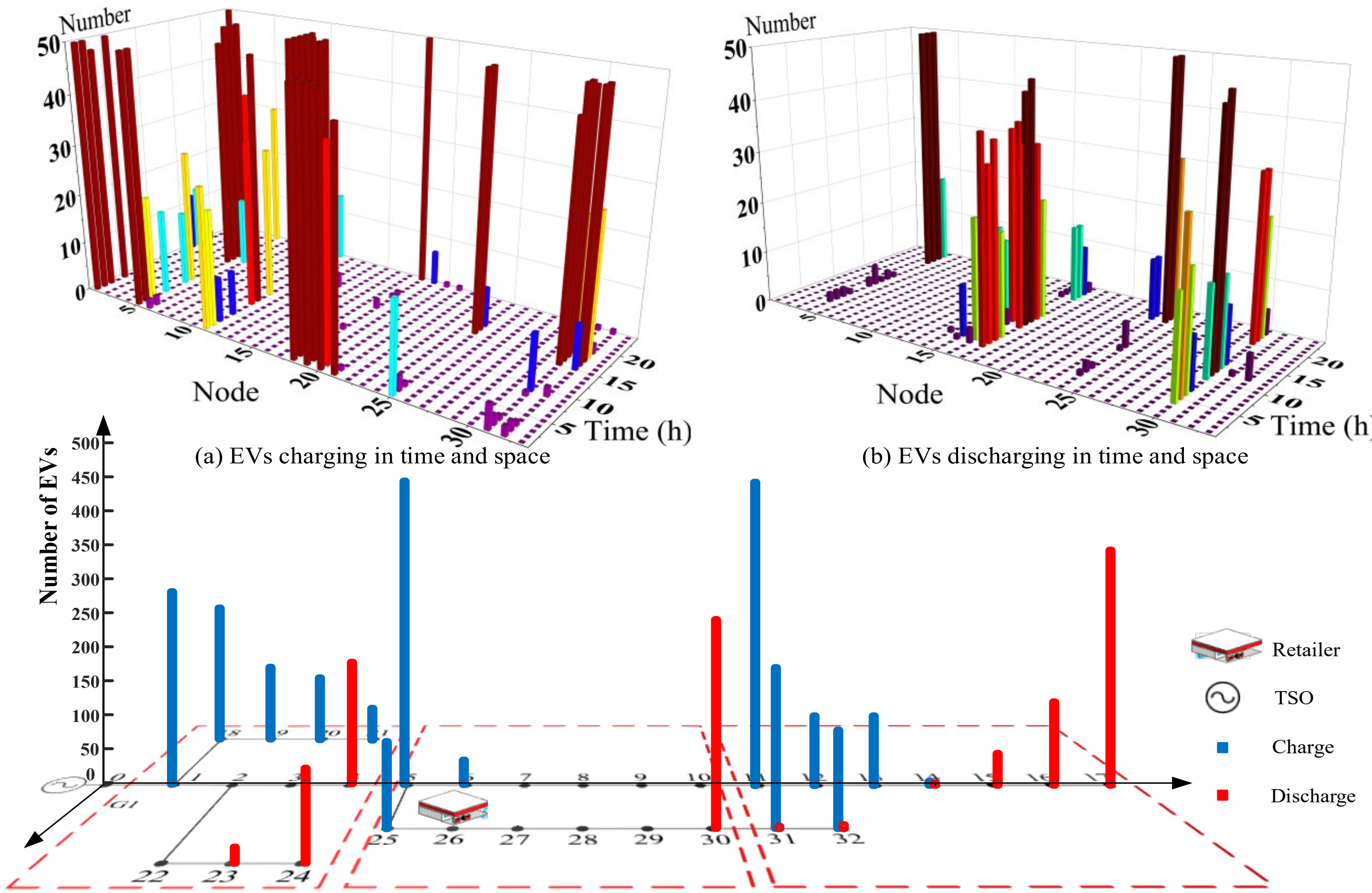

Fig. 10. The result of EV charging and discharging schedule in Test 10.

The voltage distribution of each node in the distribution network is shown in Fig. 11. It is not difficult to observe that the voltage gradually decreases from the slack node to the end node. The voltage distribution of all nodes in Test 10, where EVs are considered, is more even than that in Test 9 (without EVs), highlighting the role of EVs as flexible energy storage in achieving a more even power distribution in the network.

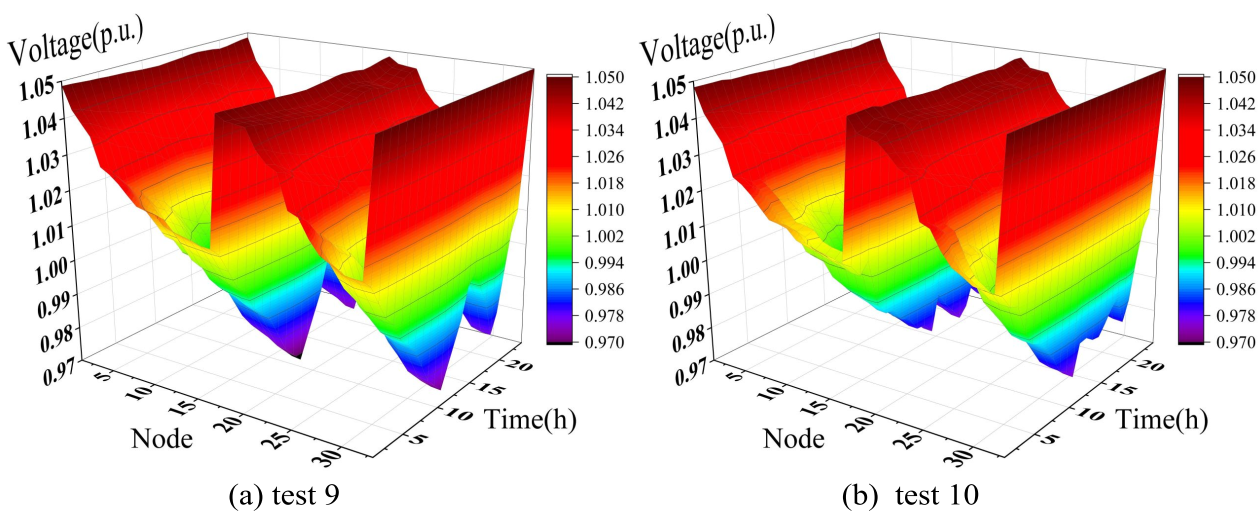

Fig. 11. Voltage of different nodes (Tests 9-10).

The network losses of the distribution network under the two tests are shown in Fig. 12. Comparing the network loss curves of Tests 9 and 10 with the spatial distribution of EV charging and discharging loads in Fig. 10(c), for example, during the period of 8:00 p.m. to 11:00 p.m., the network losses of Test 10 are smaller than those of Test 9. This is because the night charging load of Test 10 is closer to the slack bus than that of Test 9 without EVs (zero charging load). The same applies to other periods. In summary, it can be concluded that network losses increase when EVs are charging (with a smaller increase in losses closer to the slack bus) and decrease when EVs are discharging (with a smaller decrease in losses closer to the slack bus). The total network losses of Tests 9 and 10 are 2.5256 MW and 2.4974 MW, respectively. The total network losses of Test 10 are smaller than those of Test 9, which is because Test 10 has EVs charging near the slack bus and discharging near the end nodes, resulting in a smaller voltage difference between the slack bus and end nodes.

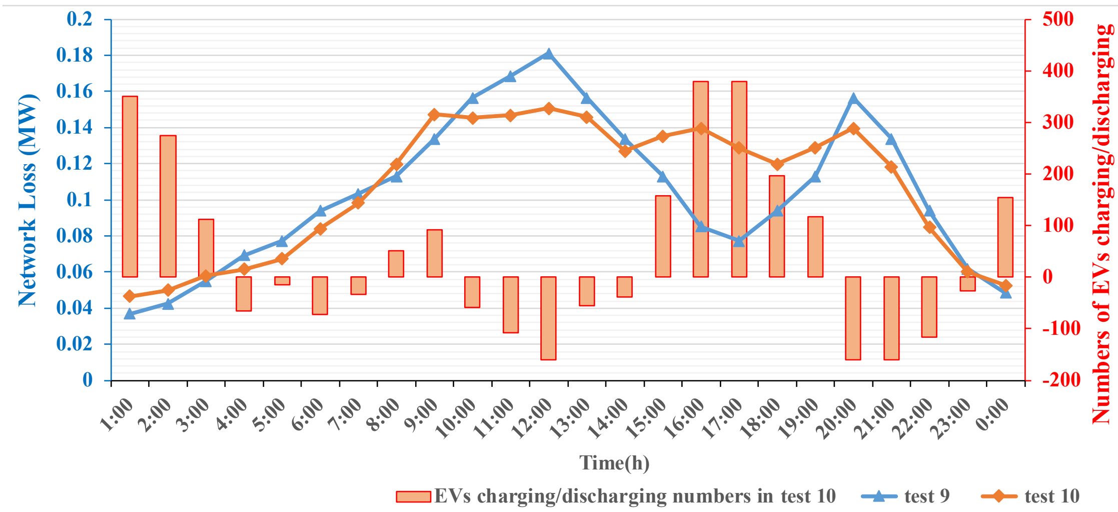

Fig. 12. The network loss curve of the distribution network (Tests 9-10).

3.4 Discussion

To further scrutinize the effectiveness of the robust pricing strategy and hybrid demand response mechanism proposed in this paper, this section conducts separate discussions on the clustering methods employed for real-time DLMP and EV uncertainty within the robust pricing strategy. Regarding the hybrid demand response mechanism, the sensitivity analysis is performed to delve deeper into the robustness of the IBDR mechanism.

3.4.1 Sensitivity analysis of the incentive-based demand response mechanism

To further analyze the robustness and rationality of the IBDR mechanism between EV retailers and TDNs, which is the second part of the proposed hybrid DR mechanism, the section continues to analyze the results of Test 7. The impact of CM_j on scheduling is listed in Table 5. The result shows that the total value of saved energy varies from 2540 MWh to 2820 MWh and represents the sensitivity of the optimal solution to CM_j. As shown in Table 5, it is not difficult to find that as the agreed amount of energy reduction by EV retailers increases, retailers will reduce more energy, and the incentives will also increase.

Table 5. Effect of Varying CM_j on the network.

EV retailers	CM_1	CM_2	CM_3	CM_4	CM_5
Total Retailers Curtailed (MWh)	2540.00	2610.00	2680.00	2750.00	2820.00
Total Retailers Incentive (￥)	645144.04	654625.26	722514.33	758311.91	853723.77

Fig. 13 illustrates the load reduction and corresponding incentives obtained by each EV retailer. It is evident that EV retailers with the highest willingness to reduce their load have achieved the greatest reduction and also received the highest compensation. EV retailer 7, which reduced the most load, received more incentives than other EV retailers who reduced less load. This result highlights the value of the IBDR mechanism for EV retailers. Full details of the default case's (CM_3) results are shown in Appendix G (Table G.2, which shows the power curtailed by all EV retailers, and Table G.3, which shows the incentives received by all EV retailers).

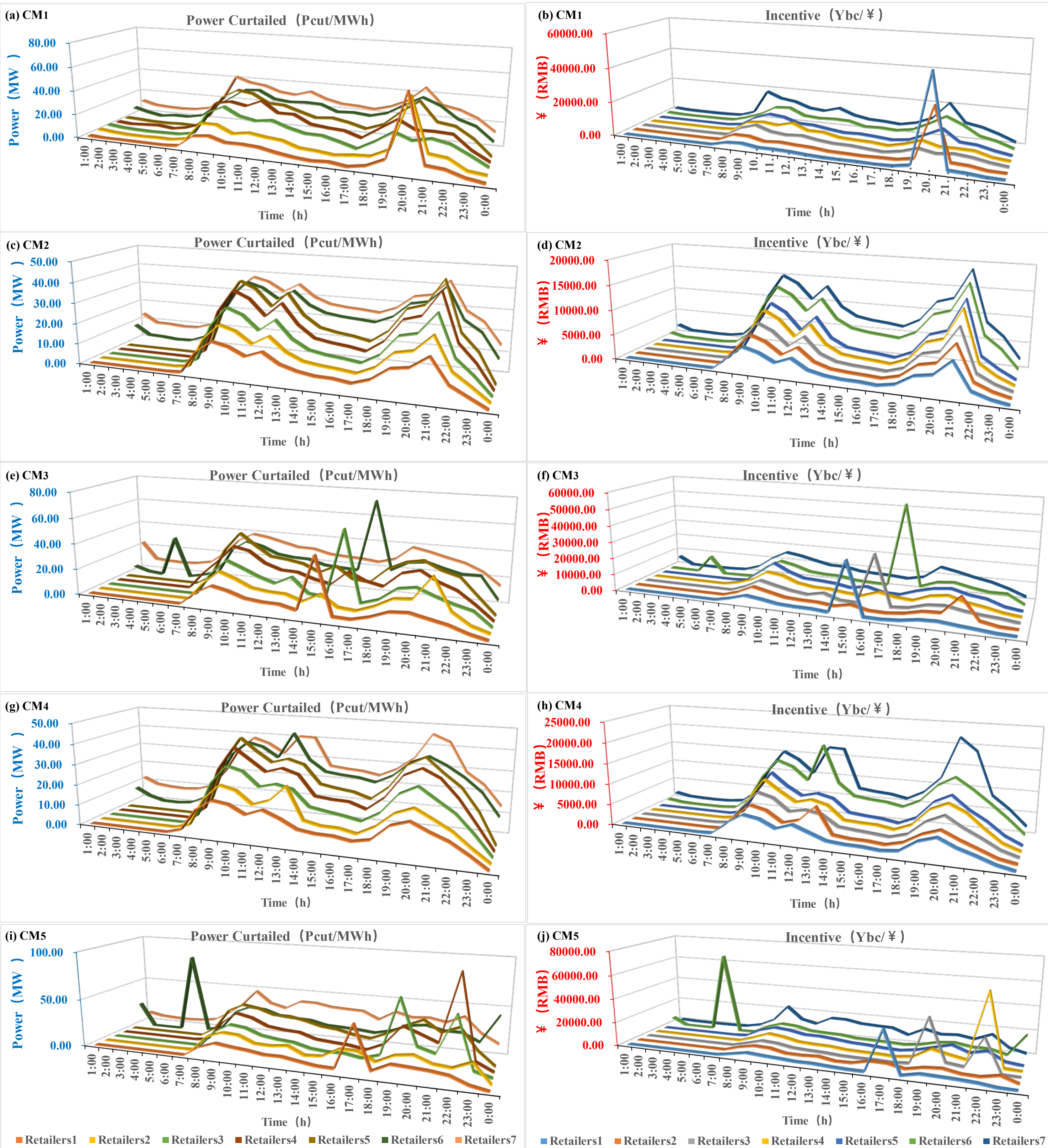

Fig. 13. EV retailers power curtailed and incentives.

3.4.2 Computational performance of the robust pricing strategy

The objective pursued by EV retailers involves formulating an alternative mixed-integer programming for the robust pricing strategy, denoted herein as MIP-RS. The computational performance is a key factor for the real application of the proposed two-stage robust pricing strategy. In this section, computational performance evaluation of MIP-RS is conducted alongside two comparable solutions, namely the PSO robust pricing strategy (PSO-RS) and the mixed-integer nonlinear programming for the robust pricing strategy (MINP-RS). Notably, MINP-RS deviates from the MIP-RS proposed in this article by its omission of handling bilinear terms such as $\mu_t^{Da} P_{b,t}^{Da}$ in Appendix D.1. PSO-RS method utilizes intelligent algorithms to solve robust pricing strategy models.

Table 6 provides evidence of the superiority of MIP-RS over alternative approaches, substantiated by its superior achievement in total operational cost. Furthermore, to gauge the impact of problem size on computational performance, MIP-RS, PSO-RS, and MINP-RS have also been applied to the original IEEE 33 system and to systems comprising up to IEEE 69 system that were created in the same way as the IEEE 118. Table 6 presents the computation times required by each method to attain a solution meeting a 0.5% optimality tolerance. As indicated in Table 6, the three approaches generally exhibit increased computation times with an escalating number of nodes. Nonetheless, several noteworthy aspects merit consideration.

Table 6. Comparison of computational dimension and results.

Network	Parameter		MIP-RS	MINP-RS	PSO-RS	Optimal method
IEEE 33	Computing time (s)	Solve AC-OPF	252.529	>5h	486.272	MIP-RS
		MIP	8.349			
	Total operation cost (RMB)		151.926	145.864	150.524	MIP-RS
IEEE 69	Computing time (s)	Solve AC-OPF	532.394	>10h	958.238	MIP-RS
		MIP	17.839			
	Total operation cost (RMB)		165.373	158.594	161.587	MIP-RS
IEEE 118	Computing time (s)	Solve AC-OPF	470.875	>24h	1391.058	MIP-RS
		MIP	5.051			
	Total operation cost (RMB)		178.725	159.477	174.291	MIP-RS

Notes: Given the independence among retailers, all distribution networks are assumed to include only one EV retailer, and the daily service quantity of EVs by the retailer aligns with the description in Section 3.1.

1) The computation time of MIP-RS is primarily devoted to solving the AC power flow model to obtain dual variables (see Appendix D.1.3). With the model's bilinear terms handled, the computation time is only 8.349s. In contrast, MINP-RS, due to the presence of bilinear terms, requires a minimum solving time of 1 hour, and this time sharply increases with the number of nodes, even reaching a point where it becomes infeasible to solve. Although the computation time of PSO-RS is slightly longer than the proposed method in this paper, it is challenging to ensure the attainment of a globally optimal solution.

2) The determination of a clear increase ratio in computing time is challenging. The computation time of the robust pricing strategy is influenced by various factors, particularly the problem structure. This complexity may result in somewhat unexpected outcomes, as exemplified by the shorter computing time taken by MIP-RS for IEEE 118 compared to the computing times required for IEEE 69.

3) Compared to PSO-RS and MINP-RS, MIP-RS features a convex optimization problem, ensuring computation time that meet the dispatching requirement of power grid (every 15 minutes). However, for large-scale node networks, the computation time of PSO-RS is challenging to meet scheduling requirements.

Irrespective of the problem size, MIP-RS reaches a solution satisfying the specified optimality gap in a shorter time than PSO-RS and MINP-RS.

4 Conclusion

To ensure economic benefits for DSOs, TSO, EV retailers, and EV users, as well as to incentivize EV users and EV retailers to participate in the energy management of TDNs, this paper proposes a bi-level EV co-optimization strategy based on the robust pricing strategy and hybrid DR mechanisms for both EV users and EV retailers. Based on the simulation results, the following conclusions can be drawn:

(1) Within the coverage area of the transmission network, the proposed bi-level optimization strategy based on robust pricing can adapt to the requirements of grid planning, power generation, and hybrid DR scenarios by optimizing the charging and discharging plans of EVs in time and space. This strategy can improve the economic efficiency of the power grid (the IBDR benefit is 509854.000 ￥), stimulate the IBDR incentives of EV retailers (as the willingness of EV retailers to reduce load increased from 0 to 1, the economic benefits obtained increased from 59958.089 ￥ to 180535.287 ￥; compared to Test 1, with the increase in the number of EVs, the revenue of EV retailers under Test 4 has increased by 4%), and increase the benefits of EV users through PBDR (the PBDR benefit is 10.709 ￥ under proportional reduction).

(2) The distributed robust optimization idea of price used in this paper is driven by actual data and considers both the optimality and conservatism of robust optimization, avoiding the problem of being overly conservative and sacrificing economic efficiency (the proposed robust pricing strategy can achieve a higher average revenue compared to the deterministic optimization strategy, 10.709 ￥ in comparison with 8.703 ￥). From the perspective of long-term operation, the results obtained through robust optimization can adapt to more uncertain scenarios and enhance the expected benefits of all EV users within the distribution network coverage area.

(3) The IBDR mechanism for EV retailers proposed in this paper can meet the incentive requirements of EV retailers. The incentives obtained by EV retailers are consistent with their willingness to reduce loads. The relationship between the interruption value and the incentive for EV retailers is positively correlated. When the interruption value of EV retailers increases from 2540 MWh to 2820 MWh, the corresponding incentives for the same power also decrease (from 645144.04 MWh to 853723.77 MWh).

(4) The hybrid DR mechanism for EV retailers proposed in this paper and the EV charging and discharging plan under the co-optimization of TDNs can achieve peak shaving and valley filling. As seen from Fig. 6, the higher the EV penetration rate, the higher the system cost. Compared to a constant price in Test 2, a fluctuating price in Test 4 can help smooth out the output power of units.

(5) The total network losses of Tests 9 and 10 are 2.5256 MW and 2.4974 MW, respectively. At the distribution network level, measures such as increasing the voltage level at the end nodes, arranging EVs to charge at step-down substations, discharging at end nodes, installing step-down transformers in residential areas, and setting up end nodes in office buildings can be taken to reduce network losses.

With high uncertainties in electricity consumption and prices, compared with separate scheduling either in the transmission or distribution network, the proposed bi-level strategy can satisfy the economic and safety objectives of all participants, including grid operators, EV retailers, and EV users. This research may shed light on future studies on the DR mechanisms for both EV retailers and EV users in TDNs from the perspective of economic strategy. The profitability of all participants in the market is guaranteed. The simultaneous participation of EV retailers and EV users in TDNs' operations can make full use of the flexibilities of large-scale EVs, which relieves the adverse impact of renewable energy volatility and congestion problems on the power grid.

Future work will focus on improving the speed of UC operations in the day-ahead stage to better meet the update rate of grid scheduling. Besides, in the TDNs, considering the high proportions of DERs, EV users' privacy concerns and incentive inadequacy, and an in-depth modeling method for the uncertain characteristics of EVs, the energy sharing mechanism with EV retailers and the penalty mechanism for EV retailer's IBDR mechanism will be considered in future work. With more efficient and sufficient methods of energy management, the operation of transmission and distribution systems with high DERs will be economical and sustainable, which contributes to reducing carbon emissions, ensuring system stability, and achieving economically efficient operations across the entire coverage area.

Declaration of competing interest

The authors declare that they have no known competing financial interests or personal relationships that could have appeared to influence the work reported in this paper.

Acknowledgments

This work is supported by the National Natural Science Foundation of China under Grant 52177204; and the Major Science and Technology Projects in Anhui Province under Grant 202003a05020019.

Reference

[1] Nicole W. Renewables 2022 Global Status Report China Factsheet - Key Headlines. France: REN21; 2022.

[2] Lanz L, Noll B, Schmidt TS, Steffen B. Comparing the levelized cost of electric vehicle charging options in Europe. Nat Commun. 2022;13(1):5277.https://doi.org/10.1038/s41467-022-32835-7.

[3] Bibra EM, Connelly E, Dhir S, Drtil M, Henriot P, Hwang I, et al. Global EV outlook 2022: Securing supplies for an electric future. 2022.

[4] Mohseni S, Brent AC, Kelly S, Browne WN. Demand response-integrated investment and operational planning of renewable and sustainable energy systems considering forecast uncertainties: A systematic review. Renew Sustain Energy Rev. 2022;158:112095.https://doi.org/10.1016/j.rser.2022.112095.

[5] Li K, Shao C, Zhang H, Wang X. Strategic Pricing of Electric Vehicle Charging Service Providers in Coupled Power-Transportation Networks. IEEE Trans Smart Grid. 2023;14(3):2189-201.https://doi.org/10.1109/TSG.2022.3219109.

[6] Powell S, Cezar GV, Min L, Azevedo IML, Rajagopal R. Charging infrastructure access and operation to reduce the grid impacts of deep electric vehicle adoption. Nat Energy. 2022;7(10):932-45.https://doi.org/10.1038/s41560-022-01105-7.

[7] Li X, Wang Z, Zhang L, Sun F, Cui D, Hecht C, et al. Electric vehicle behavior modeling and applications in vehicle-grid integration: An overview. Energy. 2023;268:126647.https://doi.org/10.1016/j.energy.2023.126647.

[8] Nizami MSH, Hossain MJ, Mahmud K. A Nested Transactive Energy Market Model to Trade Demand-Side Flexibility of Residential Consumers. IEEE Trans Smart Grid. 2021;12(1):479-90.https://doi.org/10.1109/TSG.2020.3011192.

[9] Zou W, Sun Y, Gao D-c, Zhang X, Liu J. A review on integration of surging plug-in electric vehicles charging in energy-flexible buildings: Impacts analysis, collaborative management technologies, and future perspective. Appl Energy. 2023;331.https://doi.org/10.1016/j.apenergy.2022.120393.

[10] Song D, Meng W, Dong M, Yang J, Wang J, Chen X, et al. A critical survey of integrated energy system: Summaries, methodologies and analysis. Energy Convers Manag. 2022;266:115863.https://doi.org/10.1016/j.enconman.2022.115863.

[11] Morales-España G, Tejada-Arango DA. Modeling the Hidden Flexibility of Clustered Unit Commitment. IEEE Trans Power Syst. 2019;34(4):3294-6.https://doi.org/10.1109/TPWRS.2019.2908051.

[12] Nawaz A, Wang H. Distributed stochastic security constrained unit commitment for coordinated operation of transmission

and distribution system. CSEE J Power Energy Syst. 2021;7(4):708-18.https://doi.org/10.17775/CSEEJPES.2020.02150.
[13] Wang L, Lin J, Dong H, Wang Y, Zeng M. Demand response comprehensive incentive mechanism-based multi-time scale optimization scheduling for park integrated energy system. Energy. 2023;270:126893.https://doi.org/10.1016/j.energy.2023.126893.
[14] Park S-W, Cho K-S, Hoefter G, Son S-Y. Electric vehicle charging management using location-based incentives for reducing renewable energy curtailment considering the distribution system. Appl Energy. 2022;305:117680.https://doi.org/10.1016/j.apenergy.2021.117680.
[15] Lyu X, Liu T, Liu X, He C, Nan L, Zeng H. Low-carbon robust economic dispatch of park-level integrated energy system considering price-based demand response and vehicle-to-grid. Energy. 2023;263:125739.https://doi.org/10.1016/j.energy.2022.125739.
[16] Kaur AP, Singh M. Time-of-Use tariff rates estimation for optimal demand-side management using electric vehicles. Energy. 2023;273:127243.https://doi.org/10.1016/j.energy.2023.127243.
[17] shafiei M, Ghasemi-Marzbali A. Electric vehicle fast charging station design by considering probabilistic model of renewable energy source and demand response. Energy. 2023;267:126545.https://doi.org/10.1016/j.energy.2022.126545.
[18] Wen L, Zhou K, Li J, Wang S. Modified deep learning and reinforcement learning for an incentive-based demand response model. Energy. 2020;205:118019.https://doi.org/10.1016/j.energy.2020.118019.
[19] Mohandes B, Moursi MSE, Hatziargyriou ND, Khatib SE. Incentive Based Demand Response Program for Power System Flexibility Enhancement. IEEE Trans Smart Grid. 2021;12(3):2212-23.https://doi.org/10.1109/TSG.2020.3042847.
[20] Xu B, Wang J, Guo M, Lu J, Li G, Han L. A hybrid demand response mechanism based on real-time incentive and real-time pricing. Energy. 2021;231:120940.https://doi.org/10.1016/j.energy.2021.120940.
[21] Xiangpeng Z, Jun Y, Sining H, Ting Z, Fuzhang W, Shouwen L. Two-stage Market Bidding Strategy of Charging Station Considering Schedulable Potential Capacity of Electric Vehicle. Automat Electric Power Syst. 2021;45(10):86-96.
[22] Zhu X, Sun Y, Yang J, Zhan X, Wu F, Fan H, et al. Hierarchical management strategy for electric vehicles charging schedule considering the scarcity of charging resources. IET Gener, Transm & Distrib. 2022;16(15):3092-108.https://doi.org/10.1049/gtd2.12503.
[23] Yang J, Wiedmann T, Luo F, Yan G, Wen F, Broadbent GH. A Fully Decentralized Hierarchical Transactive Energy Framework for Charging EVs With Local DERs in Power Distribution Systems. IEEE Trans Transp Electrific. 2022;8(3):3041-55.https://doi.org/10.1109/TTE.2022.3168979.
[24] Najafi A, Jasiński M, Leonowicz Z. A hybrid distributed framework for optimal coordination of electric vehicle aggregators problem. Energy. 2022;249:123674.https://doi.org/10.1016/j.energy.2022.123674.
[25] Xiang Y, Xue P, Wang Y, Xu L, Ma W, Shafie-Khah M, et al. Distributionally robust expansion planning of electric vehicle charging system and distribution networks. CSEE J Power Energy Syst. 2023:1-12.https://doi.org/10.17775/CSEEJPES.2021.08540.
[26] Perez-Diaz A, Gerding E, McGroarty F. Coordination and payment mechanisms for electric vehicle aggregators. Appl Energy. 2018;212:185-95.https://doi.org/10.1016/j.apenergy.2017.12.036.
[27] Li H, Wan Z, He H. Constrained EV Charging Scheduling Based on Safe Deep Reinforcement Learning. IEEE Trans Smart Grid. 2020;11(3):2427-39.https://doi.org/10.1109/TSG.2019.2955437.
[28] Wang L, Zhu Z, Jiang C, Li Z. Bi-Level Robust Optimization for Distribution System With Multiple Microgrids Considering Uncertainty Distribution Locational Marginal Price. IEEE Trans Smart Grid. 2021;12(2):1104-17.https://doi.org/10.1109/TSG.2020.3037556.
[29] Kandpal B, Pareek P, Verma A. A robust day-ahead scheduling strategy for EV charging stations in unbalanced distribution grid. Energy. 2022;249:123737.https://doi.org/10.1016/j.energy.2022.123737.
[30] Xiangpeng Z, Jun Y, Xinyan W, Yimin S, Xiaorui Q, Fuzhang W. Robust Pricing Strategy of Power Retailer Considering Linkage of Real-time Market. Power System Technology. 2022;46(06):2141-53.https://doi.org/10.13335/j.1000-3673.pst.2021.2157.
[31] Ai X, Wu J, Hu J, Yang Z, Yang G. Distributed congestion management of distribution networks to integrate prosumers

energy operation. IET Gener, Transm & Distrib. 2020;14(15):2988-96.https://doi.org/10.1049/iet-gtd.2019.1110.
[32] Wang Y, Qiu J, Tao Y. Robust energy systems scheduling considering uncertainties and demand side emission impacts. Energy. 2022;239:122317.https://doi.org/10.1016/j.energy.2021.122317.
[33] Yang Z, Yang F, Min H, Tian H, Hu W, Liu J, et al. Energy management programming to reduce distribution network operating costs in the presence of electric vehicles and renewable energy sources. Energy. 2023;263:125695.https://doi.org/10.1016/j.energy.2022.125695.
[34] Zhang X, Wang Z, Lu Z. Multi-objective load dispatch for microgrid with electric vehicles using modified gravitational search and particle swarm optimization algorithm. Appl Energy. 2022;306:118018.https://doi.org/10.1016/j.apenergy.2021.118018.
[35] Yin W, Qin X. Cooperative optimization strategy for large-scale electric vehicle charging and discharging. Energy. 2022;258:124969.https://doi.org/10.1016/j.energy.2022.124969.
[36] Yin W, Wen T, Zhang C. Cooperative optimal scheduling strategy of electric vehicles based on dynamic electricity price mechanism. Energy. 2023;263:125627.https://doi.org/10.1016/j.energy.2022.125627.
[37] Du W, Ma J, Yin W. Orderly charging strategy of electric vehicle based on improved PSO algorithm. Energy. 2023;271:127088.https://doi.org/10.1016/j.energy.2023.127088.
[38] Nimalsiri NI, Ratnam EL, Mediwaththe CP, Smith DB, Halgamuge SK. Coordinated charging and discharging control of electric vehicles to manage supply voltages in distribution networks: Assessing the customer benefit. Appl Energy. 2021;291:116857.https://doi.org/10.1016/j.apenergy.2021.116857.
[39] Yin W, Ji J, Wen T, Zhang C. Study on orderly charging strategy of EV with load forecasting. Energy. 2023;278:127818.https://doi.org/10.1016/j.energy.2023.127818.
[40] Mehta R, Verma P, Srinivasan D, Yang J. Double-layered intelligent energy management for optimal integration of plug-in electric vehicles into distribution systems. Appl Energy. 2019;233-234:146-55.https://doi.org/10.1016/j.apenergy.2018.10.008.
[41] Egbue O, Uko C, Aldubaisi A, Santi E. A unit commitment model for optimal vehicle-to-grid operation in a power system. Int J Electr Power Energy Syst. 2022;141:108094.https://doi.org/10.1016/j.ijepes.2022.108094.
[42] Solanke TU, Khatua PK, Ramachandaramurthy VK, Yong JY, Tan KM. Control and management of a multilevel electric vehicles infrastructure integrated with distributed resources: A comprehensive review. Renew Sustain Energy Rev. 2021;144.https://doi.org/10.1016/j.rser.2021.111020.
[43] Lu X, Li K, Xu H, Wang F, Zhou Z, Zhang Y. Fundamentals and business model for resource aggregator of demand response in electricity markets. Energy. 2020;204.https://doi.org/10.1016/j.energy.2020.117885.
[44] Cartelle Barros JJ, de Llano Paz F, Lara Coira M, de la Cruz López MP, del Caño Gochi A, Soares I. New approach for assessing and optimising the environmental performance of multinational electricity sectors: A European case study. Energy Convers Manag. 2022;268:116023.https://doi.org/10.1016/j.enconman.2022.116023.
[45] Ma Z, Chen H, Chai Y. Analysis of voltage stability uncertainty using stochastic response surface method related to wind farm correlation. Prot Control Mod Power Syst. 2017;2(1):20.https://doi.org/10.1186/s41601-017-0051-3.
[46] Chen X, Huang L, Liu J, Song D, Yang S. Peak shaving benefit assessment considering the joint operation of nuclear and battery energy storage power stations: Hainan case study. Energy. 2022;239:121897.https://doi.org/10.1016/j.energy.2021.121897.
[47] Ehsan A, Yang Q. State-of-the-art techniques for modelling of uncertainties in active distribution network planning: A review. Appl Energy. 2019;239:1509-23.https://doi.org/10.1016/j.apenergy.2019.01.211.
[48] Gurobi Optimization L. Gurobi optimizer reference manual, version 9.5 (2022).
[49] Lehmann K, Grastien A, Hentenryck PV. AC-Feasibility on Tree Networks is NP-Hard. IEEE Trans Power Syst. 2016;31(1):798-801.https://doi.org/10.1109/TPWRS.2015.2407363.
[50] Low SH. Convex relaxation of optimal power flow—Part I: Formulations and equivalence. IEEE Trans Contr of Netw Syst. 2014;1(1):15-27.https://doi.org/10.1109/TCNS.2014.2309732.
[51] Low SH. Convex relaxation of optimal power flow—Part II: Exactness. IEEE Trans Contr of Netw Syst. 2014;1(2):177-89.https://doi.org/10.1109/TCNS.2014.2323634.
[52] Meng W, Song D, Deng X, Dong M, Yang J, Rizk-Allah RM, et al. Dynamic Optimal Power Flow of Active Distribution

Network Based on LSOCR and Its Application Scenarios. Electronics. 2023;12(7).https://doi.org/10.3390/electronics12071530.
[53] Wang H-J, Pan J-S, Nguyen T-T, Weng S. Distribution network reconfiguration with distributed generation based on parallel slime mould algorithm. Energy. 2022;244.https://doi.org/10.1016/j.energy.2021.123011.
[54] Ma XY, Sun YZ, Fang HL. Scenario Generation of Wind Power Based on Statistical Uncertainty and Variability. IEEE Trans on Sustain Energy. 2013;4(4):894-904.https://doi.org/10.1109/TSTE.2013.2256807.
[55] Nwulu NI, Xia X. Optimal dispatch for a microgrid incorporating renewables and demand response. Renew Energy. 2017;101:16-28.https://doi.org/10.1016/j.renene.2016.08.026.
[56] Chen X, Huang L, Zhang X, He S, Sheng Z, Wang Z, et al. Robust Optimal Dispatching of Wind Fire Energy Storage System Based on Equilibrium Optimization Algorithm. Front Energy Res. 2021:577.https://doi.org/10.3389/fenrg.2021.754908.
[57] Patil H, Kalkhambkar VN. Grid Integration of Electric Vehicles for Economic Benefits: A Review. J Clean Prod. 2021;9(1):13-26.https://doi.org/10.35833/MPCE.2019.000326.
[58] Jia Z, Li J, Zhang XP, Zhang R. Review on Optimization of Forecasting and Coordination Strategies for Electric Vehicle Charging. J Mod Power Syst Clean Energy. 2023;11(2):389-400.https://doi.org/10.35833/MPCE.2021.000777.